Biophysical Chemistry 156 (2011) 51–67

Contents lists available at ScienceDirect

Biophysical Chemistry

journal homepage: http://www.elsevier.com/locate/biophyschem

Hydrophobic hydration processes
Thermal and chemical denaturation of proteins

E. Fisicaro *, C. Compari, A. Braibanti

Department of Pharmacological, Biological and Applied Chem. Sciences, Physical Chemistry Section, University of Parma, I-43100 Parma, Italy

ARTICLE INFO

Article history:
Received 2 February 2011
Received in revised form 21 February 2011
Accepted 21 February 2011
Available online 3 March 2011

Keywords:
Water clusters
Cavity formation
Cavity reduction
Thermal enthalpy
Termal entropy
Motive free-energy

ABSTRACT

The hydrophobic hydration processes have been analysed under the light of a mixture model of water that is assumed to be composed by clusters $(W_5)_I$, clusters $(W_4)_{II}$ and free water molecules W_{III}. The hydrophobic hydration processes can be subdivided into two Classes A and B. In the processes of Class A, the transformation $\mathbf{A}(-\xi_w W_I \rightarrow \xi_w W_{II} + \xi_w W_{III} + \text{cavity})$ takes place, with expulsion from the bulk of ξ_w water molecules W_{III}, whereas in the processes of Class B the opposite transformation $\mathbf{B}(-\xi_w W_{III} - \xi_w W_{II} \rightarrow \xi_w W_I - \text{cavity})$ takes place, with condensation into the bulk of ξ_w water molecules W_{III}. The *thermal equivalent dilution* (*TED*) principle is exploited to determine the number ξ_w. The denaturation (unfolding) process belongs to Class A whereas folding (or renaturation) belongs to Class B. The enthalpy ΔH_{den} and entropy ΔS_{den} functions can be disaggregated in thermal and motive components, $\Delta H_{den} = \Delta H_{therm} + \Delta H_{mot}$, and $\Delta S_{den} = \Delta S_{therm} + \Delta S_{mot}$, respectively. The terms ΔH_{therm} and ΔS_{therm} are related to phase change of water molecules W_{III}, and give no contribution to free energy ($\Delta G_{therm} = 0$). The motive functions refer to the process of cavity formation (Class A) or cavity reduction (Class B), respectively and are the only contributors to free energy ΔG_{mot}. The folded native protein is thermodynamically favoured ($\Delta G_{fold} \equiv \Delta G_{mot} < 0$) because of the outstanding contribution of the positive entropy term for cavity reduction, $\Delta S_{red} \gg 0$. The native protein can be brought to a stable denatured state ($\Delta G_{den} \equiv \Delta G_{mot} < 0$) by coupled reactions. Processes of protonation coupled to denaturation have been identified. In thermal denaturation by calorimetry, however, is the heat gradually supplied to the system that yields a change of phase of water W_{III}, with creation of cavity and negative entropy production, $\Delta S_{for} \ll 0$. The negative entropy change reduces and at last neutralises the positive entropy of folding. In molecular terms, this means the gradual disruption by cavity formation of the entropy-driven hydrophobic bonds that had been keeping the chains folded in the native protein. The action of the chemical denaturants is similar to that of heat, by modulating the equilibrium between W_I, W_{II}, and W_{III} toward cavity formation and negative entropy production. The salting-in effect produced by denaturants has been recognised as a hydrophobic hydration process belonging to Class A with cavity formation, whereas the salting-out effect produced by stabilisers belongs to Class B with cavity reduction.
Some algorithms of denaturation thermodynamics are presented in the Appendices.

1. Introduction[1]

We have studied [1–3] the thermodynamics of the solubility in water of non-polar gases in comparison with the thermodynamics of micelle formation in water. The analysis has been pursued on the basis of a structure model (FCB model) for water. The FCB model assigns to water three structures consisting of clusters $(W_5)_I$, clusters $(W_4)_{II}$ and free water molecules W_{III}, respectively. Release of ξ_w water molecules W_{III} from W_I produces water W_{II} and creates a cavity to host the solute molecule. In the solution, W_I (low density) forms the bulk, W_{II} (high density) forms a sheath around the solute molecule and W_{III} are free water molecules.

The FCB model has allowed the interpretation of every hydrophobic hydration process [4] by considering that each process, although apparently different from one another, refers to a unique transformation of water clusters, direct or inverse.

The hydrophobic hydration processes can be subdivided into two Classes A and B (Fig. 1). In the processes of Class A, the transformation **A** $(-\xi_w W_I \rightarrow \xi_w W_{II} + \xi_w W_{III} + \text{cavity})$ takes place, with expulsion from the bulk of ξ_w water molecules W_{III}, whereas in the processes of Class B the opposite transformation $\mathbf{B}(-\xi_w W_{III} - \xi_w W_{II} \rightarrow \xi_w W_I - \text{cavity})$ takes place, with condensation into the bulk of ξ_w water molecules W_{III}, ("−cavity" is equivalent to cavity reduction).

The number ξ_w depends on the size of the reactant molecules. The value of ξ_w has been calculated from the slope ΔC_p of the plot

* Corresponding author. Tel.: +39 0521905028; fax: +39 0521 905026.
E-mail address: fisicaro@unipr.it (E. Fisicaro).
[1] For symbols see **Glossary** after **References**.

0301-4622/$ – see front matter © 2011 Elsevier B.V. All rights reserved.
doi:10.1016/j.bpc.2011.02.009

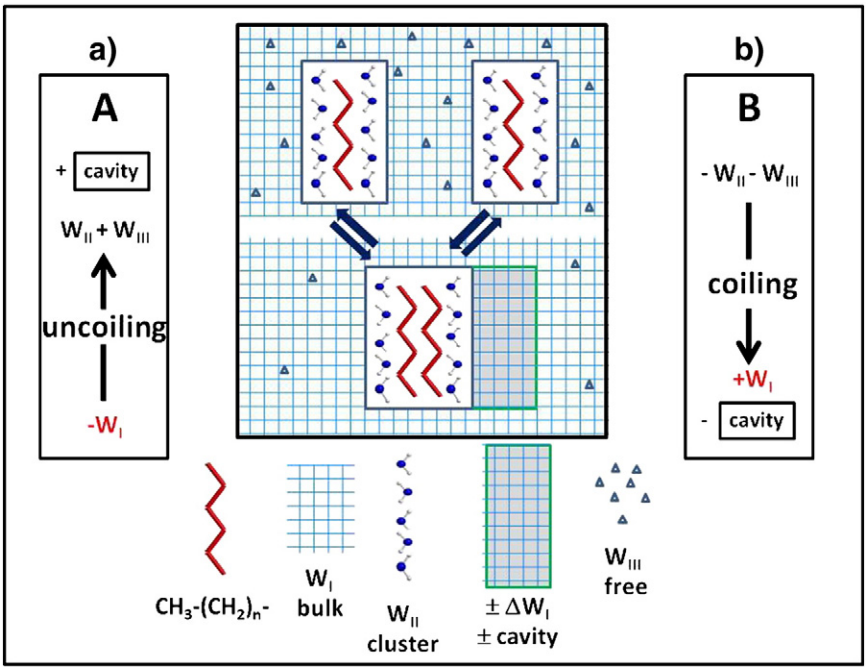

Fig. 1. A unique reaction, involving water, either direct ((left, Class A)) or inverse (right, Class B) takes place in every hydrophobic hydration process:a) Unfolding (Class A): transformation A($-\xi_w W_I \rightarrow \xi_w W_{II} + \xi_w W_{III}$ + cavity), with melting of ξ_w water molecules W_{III}b) Folding (Class B): transformation B($-\xi_w W_{III} - \xi_w W_{II} \rightarrow \xi_w W_I -$ cavity), with condensation of ξ_w water molecules W_{III}.Cavity expansion or reduction ($\pm \Delta W_I$, in grey) is proportional to ξ_w. Note, please, that the sum of white and grey areas at the bottom equals the sum of the separated white areas at the top.

$\Delta H_{app} = f(T)$ by applying the principle of *thermal equivalent dilution* (*TED*) [4,14] from the equality

$$\Delta C_p = \pm \xi_w C_{p,w} \quad (1)$$

where $C_{p,w} = 75.36\ J \cdot K^{-1}\ mol^{-1}$ is the isobaric heat capacity of liquid water. The sign + in Eq. (1) holds for Class A and the sign − for Class B. A large value of ΔC_p has been recognised as a typical property of all the hydrophobic hydration processes [5–8]. Moreover ΔC_p, and hence ξ_w, has been found to be linearly related to the length of the chain [5] or resulting as the summation of group contributions [7]. The ranges of ξ_w are different for small or large molecules, but the unitary (i.e. for $\xi_w = 1$) quantities for enthalpy and entropy are practically equal, respectively, independently from the total molecular size.

2. Thermal and motive functions

Some years ago, R. Lumry [9] has raised some doubts whether the thermodynamic data can be user-friendly if applied to isothermal processes. He thinks that enthalpy, internal energy, entropy and volume data are generally suspect since rarely have they been analysed so as to take the two species of water into account. He thinks also that the statements by Benzinger [10] that there might exist some hidden part of enthalpy and entropy not contributing to the free energy add more doubts to the validity of the thermodynamic functions as representative of the chemical reactions. Another word of caution about the splitting of ΔG into enthalpic and entropic contributions and its temperature dependence on the basis of oversimplified (inadequate) models of the protein interaction is launched by Winzor and Jackson [11]. The main possible reactions that, according to these authors, are linked to the proper protein transformations, could be isomerisation reactions, proton-base equilibria, or protein–ligand interactions. Another question raised by Lumry [12,13] concerns the thermodynamic functions for denaturation, enthalpy ΔH_{den} and entropy ΔS_{den}, that, according to Lumry, should be subdivided into two parts, motive (or work) and thermal (or compensative) functions.

We think, however, that the criticisms of Lumry, Winzor and Jackson should not be applicable to our treatment, because the model that we assume takes into account actually two types of water clusters, i.e. $(W_5)_I$ and $(W_4)_{II}$, as required by Lumry [9], together with free water molecules W_{III}. Moreover the problems of integration of the two thermal functions of Benzinger have been solved by us. As far as side reactions are concerned, the main side reaction that we have taken into account in micelle formation and in solubility of non-polar substances is just the change of phase of water W_{III} that can either melt by leaving water W_I or condense into W_I. The change of phase of water W_{III} has been shown to correspond exclusively to the thermal (or compensative) components of the thermodynamic functions suggested by Lumry. These thermal components can be identified as the hidden parts indicated by Benzinger. On the other hand, the motive components of Lumry can be associated to the process of cavity formation. Moreover, coupled protonation equilibria will be considered in the study of denaturation.

We now want to analyse whether the thermodynamic functions of protein denaturation and protein folding, calculated from the experimental data, conform to the same model FCB as the thermodynamic functions of Class A and Class B, respectively and how much the thermodynamic functions, free energy ΔG_{den}, enthalpy ΔH_{den} and entropy ΔS_{den}, are in qualitative or even quantitative agreement with the results obtained with the other hydrophobic hydration processes of both Classes.

The subdivision in Classes A and B has been done by analysing the type of curve presented in the free energy plot $(-\Delta G^o)/RT = \ln K = f(1/T)$ by any hydrophobic hydration process.[2] The plots of the processes of Class A (Fig. 2A) present invariably a minimum whereas the processes of Class B (Fig. 2B) show curves with a maximum. The type of curvature depends in particular on the type of cavity-change in the solvent, with cavity formation in Class A and cavity reduction in Class B.

[2] Relationships between thermodynamic functions and partition function can be found in Appendix A from Eq. (A.6) to Eq. (A.16)

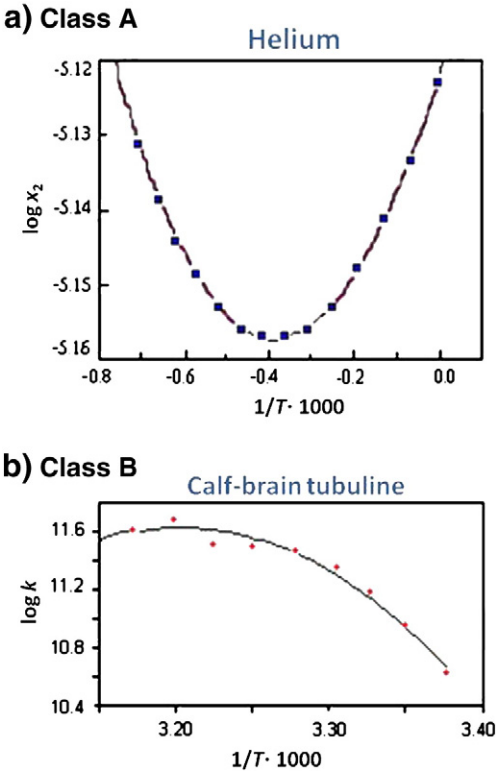

Fig. 2. Examples of free energy plots $(-\Delta G^{o})/RT = \ln K = f(1/T)$ in hydrophobic hydration processes.

A process analogous to that of gas solubility and opposite to that of micelle formation can be proposed for denaturation (Fig. 3). The hydrophobic chains previously associated in the folded protein, detach from each other and distend into the bulk of the liquid. In order to do so, they need more room and in fact a larger cavity is formed by releasing from the bulk a number ξ_w of free water molecules W_{III}. At the same time, clusters $(W_5)_I$ are transformed into clusters $(W_4)_{II}$. The equations of the equilibria involved in protein denaturation and the consequent thermodynamic relationships are developed in Appendix **A**.

We have identified as a member of Class A the process of denaturation (unfolding of the chains) and as a member of Class B the process of protein structuring (folding of the chains or renaturation, with hydrophobic bonding). The applications of this model would help us to find a rational explanation of the mechanism of both thermal and chemical denaturation of proteins.

The equilibrium denatured/native is ruled by a dissociation constant K_{den}. The free energy function

$$\left(-\Delta G_{den}\right) / RT = \ln K_{den} = f(1/T) \tag{2}$$

is represented, as well as any other process of Class A, by a curve with a minimum. This shape of the curve means that the tangent to the curve of Eq. (2), given by the van't Hoff equation

$$\partial(\ln K_{den}) / \partial(1/T) = -\Delta H_{den} / R \tag{3}$$

is changing from a negative slope at the left of the minimum to a positive slope at the right of the minimum. By calculating the derivative at any temperature of the interval, by changing sign, and by plotting ΔH_{den} against T, we obtain, for every process of Class A, a linear expression

$$\Delta H_{den} = \Delta H_{(0)} + \Delta C_p T \tag{4}$$

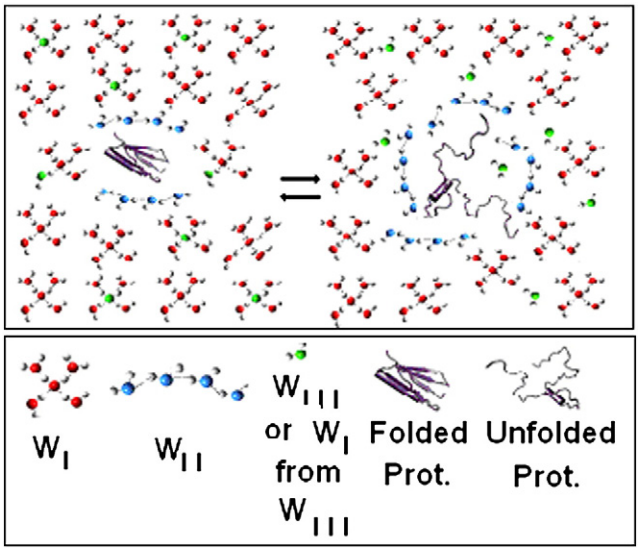

Fig. 3. Mechanism of unfolding of a protein.

with intercept $\Delta H_{(0)} < 0$ and slope $\Delta C_p > 0$. By applying *TED* [4,14] we can set

$$\Delta C_p = \xi_w C_{p,w} \tag{5}$$

where $C_{p,w}$ is the isobaric heat capacity of liquid water. Both intercept $\Delta H_{(0)}$ and slope ΔC_p are different for each compound of any type of process because they both are linear functions of the same ξ_w.

Eq. (4) is suited to distinguish the two components, motive and thermal, respectively, that form the thermodynamic functions according to the suggestions of Lumry [12,13]. The denaturation enthalpy ΔH_{den}, in fact, can be seen as composed of two parts, thermal part ΔH_{therm} and motive part ΔH_{mot}:

$$\Delta H_{den} = \Delta H_{mot} + \Delta H_{therm} \tag{6}$$

with $\Delta H_{mot} \equiv \Delta H_{(0)}$ (i.e. the intercept $\Delta H_{(0)}$ of Eq. (4)). The thermal part ΔH_{therm}, by comparison with Eq. (4) and Eq. (5),

$$\Delta H_{therm} = + \xi_w C_{p,w} T \tag{7}$$

results to be attributable exclusively to the thermal energy gained by ξ_w water molecules W_{III} removed from the bulk of the solvent and moving in the interstices.

The motive (or work) part ΔH_{mot} is composed of two terms

$$\Delta H_{mot} = \left(\Delta H_0^{(\xi_w = 0)} + \Delta H_{for}\right) = \left(\Delta H_0^{(\xi_w = 0)} + \xi_w \cdot \Delta h_{for}\right) \tag{8}$$

thus showing that ΔH_{mot} is independent from the temperature but depends on factors attaining strictly to the cavity formation of size ξ_w (ΔH_{for}) and to the affinity or repulsion between hydrophobic moieties $(\Delta H_0^{(\xi_w = 0)})$.

By plotting the denaturation entropy against $\ln T$, we obtain a straight line

$$\Delta S_{den} = \Delta S_{(0)} + \Delta C_p \ln T \tag{9}$$

where the slope ΔC_p (cf. Eq. (5)) is exactly the same obtained from the plot $\Delta H_{den} = f(T)$ for the same compound. It is thus possible to represent the entropy as composed of two parts, thermal part ΔS_{therm} and motive part ΔS_{mot}

$$\Delta S_{den} = \Delta S_{mot} + \Delta S_{therm} \tag{10}$$

with $\Delta S_{mot} \equiv \Delta S_{(0)}$ (i.e. the intercept $\Delta S_{(0)}$ of Eq. (9)). The thermal entropy ΔS_{therm} is identified as

$$\Delta S_{therm} = + \xi_w C_{p,w} \ln T \tag{11}$$

that is attributable exclusively to the thermal entropy gained, starting from the resting state of the condensed structure (at $\ln T = 0$), by ξ_w water molecules W_{III} removed from the bulk of the solvent and moving in the interstices. The motive entropy, composed by two terms,

$$\Delta S_{mot} = \left(\Delta S_0^{(\xi_w = 0)} + \Delta S_{for}\right) = \left(\Delta S_0^{(\xi_w = 0)} + x_w \cdot \Delta s_{for}\right) \tag{12}$$

is independent from the temperature: ΔS_{for} is related to the process of cavity formation and $\Delta S_0^{(\xi_w = 0)}$ refers to some configurational (concentration) change of the macromolecule as a whole.

The thermal enthalpy of Eq. (7) and the thermal entropy of Eq. (11) are related each other by the relationship

$$\Delta H_{therm} / T = \Delta S_{therm} \tag{13}$$

whereby the reaction of water molecules W_{III}, that are moving from the resting structured state to the disordered fluid state, shows a behaviour similar to a phase change, like as a melting process. The heat supplied to the melting molecules is transformed into kinetic energy of the same molecules in the fluid phase. The only difference is that, while the melting process takes place, under constant pressure, at a definite constant temperature, Eq. (13) is valid at any temperature we perform the experiment. Another point that deserves attention is the correspondence of the thermal parts of enthalpy ($+\xi_w C_{p,w} T$) and entropy ($\xi_w C_{p,w} \ln T$) with the two integrals proposed by Benzinger [10], $\Delta S^\circ_T = \int \Delta C_p dT$ and $\Delta \Gamma^\circ_T = \int (\Delta C_p / T) dT$, respectively. The importance of these hidden functions in thermodynamics of protein unfolding had been underlined by Benzinger himself.

3. Denaturation free energy as a function of temperature and pH

Free energy data for the denaturation at different temperatures have been reported by R. Lumry et al. [12]. The proteins examined by them were chymotrypsinogen A (CGN), its dimethionine sulfoxide derivative (DMSCGN), diphenyl-carbamyl-α-chymotrypsin (DPC-α-CT), and ribonuclease (RNase). The advancement of the reaction was followed spectrophotometrically. Particular care has been devoted by the Authors to the reversibility of the transitions. The following questions have been discussed by them: (1) Because of the arbitrariness introduced by the choice of the mathematical interpolation, can one obtain accurate heat-capacity information about unfolding reactions of proteins from thermal equilibrium studies? (2) What empirical equation best describes quantitatively the thermodynamic information about unfolding transitions? Analysis of data of conformational transitions is simple only if the transitions can be approximated by a two state model. Aggregation is strongly dependent on temperature, pH, protein and salt concentration. A special problem has arisen in the determination of the spectrophotometric baseline. They conclude that the errors generated by the uncertainty in the baseline at the foot and top of two different transition curves are largest and only values of ΔH_{den} and T near the middle of the transitions (around $\Delta G = 0$) present a high degree of consistency among the proteins of the chymotrypsinogen family. The result of RNase were obtained with considerable accuracy. The Authors have verified that the dependence of ΔH_{den} upon pH does not involve ΔC_p and therefore the data obtained at pH 2.8 or other pH levels could be readily corrected to pH 2. The variations of the free energy functions with pH are examined in detail in Appendix B. How it is possible to construct for each protein, a unique cumulative curve for free energy (and of course for log K_{den}) starting from sets of experimental values obtained at different pH levels is also shown there. An example of curve of log K_{den} for DMSCGN as

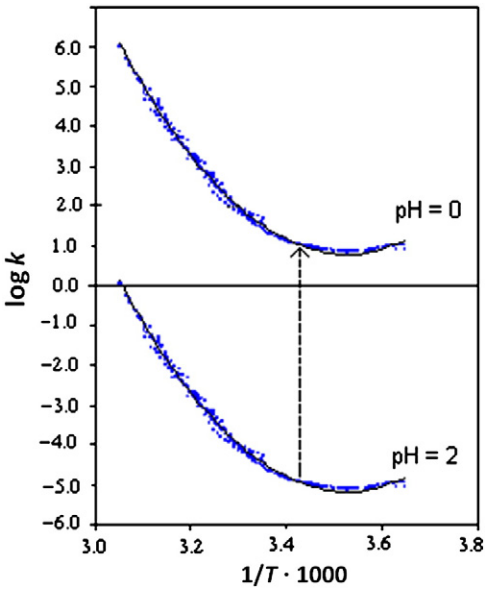

Fig. 4. Cumulative curve of log K_{den} for DMSCGN (dimethionine sulfoxide derivative of chymotrypsinogen) with all the branches displaced to pH = 2. Parallel displacement to pH = 0 brings the whole curve in the positive range of log K_{den} ($\Delta G_{den} < 0$) where the denatured state is stable.

normalised to pH = 2 (Fig. 4) shows that the values of log K_{den} lay in the range of the negative values (log $K_{den} < 0$, $\Delta G_{den} > 0$). The denatured state is, therefore, thermodynamically unstable. The curve at pH = 2, however, can be displaced parallel to itself by changing pH from pH = 2 to pH = 0. The cumulative curve moves thus to the field of the positive values (log $K_{den} > 0$, $\Delta G_{den} < 0$), thus showing that the denatured state has become thermodynamically favoured. This explains the action of proton as denaturant. Actually we have used the normalised cumulative sets obtained from the original data of Lumry [12] for the four proteins to calculate ΔH_{den} and ΔS_{den}. The equations representing the cumulative curves are reported in Table 1.

The values of ΔH_{den} for different proteins, obtained from the curves log K_{den} as the function of $(1/T)$, plotted against T, produce linear plots, as expected (Fig. 5). The values of ΔS_{den} have been calculated by the Helmholtz–Gibbs equation and then plotted against $\ln T$, thus obtaining linear plots, with the same slopes $\Delta C_p = \xi_w C_{pw}$ found for enthalpy (Fig. 6). The equations corresponding to each compound are reported in Table 2. The values of the numbers $\xi_w(S)$ calculated from the entropy plot are practically equal to those $\xi_w(H)$ obtained from the enthalpy plots. The values of ξ_w obtained are reasonable because they are much larger than those found in the solubility of non-polar substances and in micelle formation but are as large as those found in other proteins, as calculated either by equilibrium or calorimetric determinations.

The values of the motive functions (cf. Eq. (8) and Eq. (12)) can be, on their turn, disggregated in two terms, the first referring to the inter-chain interaction and the second to the process of cavity formation

Table 1
Equations representing the cumulative curves at pH = 2.

Protein	Equation	Points	R^2
CGN	$\log K_{den} = -37.458\ (1/T)^3 + 388.76\ (1/T)^2 - 1355.8\ (1/T) + 1584.6$	147	0.9985
DMSCGN	$\log K_{den} = -0.9549\ (1/T)^3 + 33.161\ (1/T)^2 - 198.21\ (1/T) + 327.86$	301	0.9947
DPCTα	$\log K_{den} = -14.750\ (1/T)^3 + 190.65\ (1/T)^2 - 793.71\ (1/T) + 1072.8$	141	0.9982
RNase	$\log K_{den} = -6.4058\ (1/T)^3 + 76.173\ (1/T)^2 - 307.71\ (1/T) + 416.62$	92	0.9996

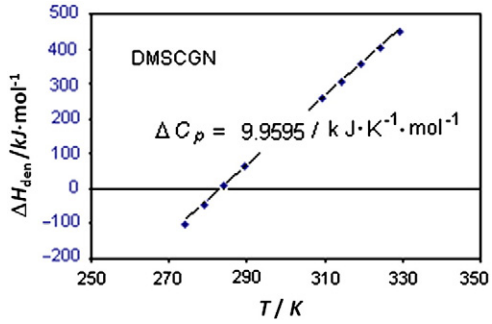

Fig. 5. Example of plot $\Delta H_{den} = f(T)$ (DMSCGN, dimethionine sulfoxide derivative of chymotrypsinogen).

(Table 3). The value for enthalpy $\Delta h_{for} = -22.5\ \mathrm{kJ \cdot mol^{-1} \cdot \xi_w^{-1}}$ is the unitary enthalpy change for the transformation from clusters $(W_5)_I$ to clusters $(W_4)_{II}$ with cavity formation, for each water molecule W_{III} released. The partial reaction of cavity formation is, therefore, exothermic. The unitary enthalpy is very close to $\Delta h_{for} = -21.6\ \mathrm{kJ \cdot mol^{-1} \cdot \xi_w^{-1}}$ found in the solubility of non-polar substances for the same process and, with change of sign, to $\Delta h_{red} = +23.2\ \mathrm{kJ \cdot mol^{-1} \cdot \xi_w^{-1}}$ for the opposite process of micelle formation with cavity reduction. For the entropy of cavity formation, we find the unitary value $\Delta s_{for} = -424.2\ \mathrm{J \cdot K^{-1} \cdot mol^{-1} \cdot \xi_w^{-1}}$ indicating the loss of entropy for cavity formation for each water molecule W_{III} released. This can be compared with $\Delta s_{for} = -445\ \mathrm{J \cdot K^{-1} \cdot mol^{-1} \cdot \xi_w^{-1}}$ found for the same process in the solubilisation of non polar sustances. It is also very similar, with change of sign, to the opposite process of cavity reduction in micelle formation $\Delta s_{red} = +433\ \mathrm{J \cdot K^{-1} \cdot mol^{-1} \cdot \xi_w^{-1}}$.

On the whole, we can assume that these coincidences of quantities are not casual and strongly support the idea that the molecular model working for the solubilisation of non polar compounds (Class A) is valid also for the denaturation of proteins. Analogously, the model working for micelle formation (Class B) is valid for the process of protein folding or protein renaturation.

4. Denaturation: entropy-opposed process

The distinction between motive and thermal parts of the thermodynamic functions can be exploited to separate the contributions of the real chemical reaction of cavity formation or reduction from the contributions of the change of phase of water W_{III}. The latter contribution coincides with the thermal part both in Eq. (6) and Eq. (10). Following Lumry [12,13], we consider, on the grounds of

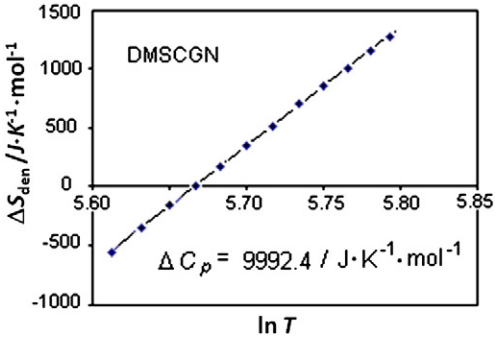

Fig. 6. Example of entropy plot. (DMSCGN, dimethionine sulfoxide derivative of chymotrypsinogen).

Table 2
Denaturation enthalpy and entropy as sum of motive and thermal components.

Compd	$\Delta H_{den} = \Delta H_{mot} + \Delta H_{therm}$		$\Delta S_{den} = \Delta S_{mot} + \Delta S_{therm}$	
	ΔH_{mot}	$\xi_w(H)\ C_{p,w}T$	ΔS_{mot}	$\xi_w(S)\ C_{p,w}\ln T$
	$\mathrm{kJ \cdot mol^{-1}}$	$\mathrm{kJ \cdot mol^{-1}}$	$\mathrm{J \cdot K^{-1} \cdot mol^{-1}}$	$\mathrm{J \cdot K^{-1} \cdot mol^{-1}}$
DMSCGN	−2823	132.2 $C_{p,w}T$	−56,615	132.6 $C_{p,w}\ln T$
CGN	−4137	191.0 $C_{p,w}T$	−81,181	189.7 $C_{p,w}\ln T$
DPCT-α	−5173	241.6 $C_{p,w}T$	−101,958	240.6 $C_{p,w}\ln T$
RNase	−1023	56.6 $C_{p,w}T$	−24,088	37.5 $C_{p,w}\ln T$

Eq. (13), that the motive parts ΔH_{mot} and ΔS_{mot} only contribute to the motive free energy ΔG_{mot}, thus obtaining a Helmholtz–Gibbs equation

$$\Delta G_{mot} = \Delta H_{mot} - T\,\Delta S_{mot} \tag{14}$$

In the denaturation of proteins, therefore, the separation of both enthalpy and entropy into thermal and motive parts is possible. The motive components have been calculated and reported in Table 4. An example is presented in Fig. 7. The diagram demonstrates that the denaturation process is thermodynamically disfavoured due to the outstanding contribution of the negative entropy change ($\Delta S_{for} \ll 0$) for cavity formation. In contrast, by attributing to the process of folding the same values of the thermodynamic functions with reversed signs, we can see (simply by changing sign to the ordinates of the diagram in Fig. 7) that the native folded state is thermodynamically favoured because entropy-driven by the prominent contribution of the positive entropy change ($\Delta S_{red} \gg 0$) of cavity reduction. The folding of the protein would seem to correspond to a decrease in entropy, but it is the positive entropy production of cavity reduction that becomes the prominent contributor to the negative motive free energy ΔG_{fold} ($\Delta G_{fold} \equiv \Delta G_{mot}$). In fact, in the process of folding, notwithstanding the protein itself is obviously more ordered in the folded state than in the unfolded one, the entropy increases, the increase deriving from the development of the reaction $\mathbf{B}(-\xi_w W_{III} - \xi_w W_{II} \rightarrow \xi_w W_I - \text{cavity})$ toward cavity reduction, with condensation into W_I of ξ_w water molecules W_{III} and production of entropy for cavity reduction (cf. $<\Delta s_{red}>_B = +432 \pm 4\ \mathrm{J \cdot K^{-1} \cdot mol^{-1} \cdot \xi_w^{-1}}$, with $\Delta S_{red} \gg 0$).

The amounts of the thermodynamic functions reported in Table 4 look very high, but this is due to the large number of interactions involved in the transformation. As a matter of fact, we must remember that the values of the thermodynamic functions associated to each unit of water W_{III} calculated either in large or small molecules are almost coincident. This fact indicates that the same type of reaction referred to one unit W_{III} is taking place both in large and small molecules.

Table 3
Motive functions: cavity formation and intra-chain interactions.

Enthalpy	Entropy
$\Delta H_{mot} = \Delta H_0^{(\xi_w = 0)} + \xi_w\,\Delta h_{for}$	$\Delta S_{mot} = \Delta S_0^{(\xi_w = 0)} + \xi_w\,\Delta s_{for}$
$\Delta H_{mot} = +205.05 - 22.5\ \xi_w$	$\Delta S_{mot} = -59.7 - 424.2\ \xi_w$

Table 4
Motive parts of the thermodynamic functions for protein denaturation.

Protein	ΔH_0	$T\,\Delta S_0$	ΔG_0 (298 K)
	$\mathrm{kJ \cdot mol^{-1}}$	$\mathrm{kJ \cdot mol^{-1}}$	$\mathrm{kJ \cdot mol^{-1}}$
DMSCGN	−2823	$T \cdot 56.62$	14,050
CGN	−4137	$T \cdot 81.18$	20,055
DPCT-a	−5173	$T \cdot 101.96$	25,096
R Nase	−1023	$T \cdot 24.09$	6156

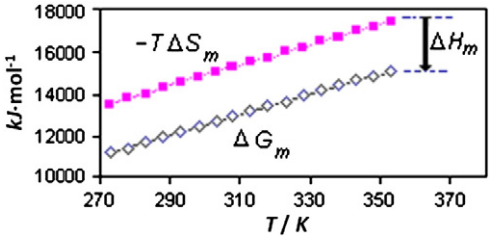

Fig. 7. Motive parts of enthalpy, entropy and free energy for protein denaturation ($\Delta H_{mot} = -2823$ kJ·mol^{-1}).

5. Coupled protonation equilibria

The denaturation enthalpy ΔH_{den} for every protein can then be represented by the general equation

$$\Delta H_{den} = \left(\Delta H_0^{(\xi_w=0)} + \Delta H_{for}\right) + \Delta H_{therm} = (+205.05 - 22.5\xi_w) + \xi_w C_{p,w} T \quad (15)$$

where the isobaric heat capacity of water is $C_{p,w} = 0.07536$ kJ·K^{-1}·mol^{-1}.

The denaturation entropy can be represented by an equation that corresponds term by term to Eq. (15), that is

$$\Delta S_{den} = \left(\Delta S_0^{(\xi_w=0)} + \Delta S_{for}\right) + \Delta S_{therm} = (-59.7 - 424.2\xi_w) + \xi_w C_{p,w} \ln T \quad (16)$$

where $C_{p,w} = 75.36$ J·K^{-1}·mol^{-1} and ξ_w indicates again the number of water molecules of type W_{III}, $\Delta S_{for} = \xi_w \Delta s_{for} < 0$ is the entropy change for cavity formation and the term $\Delta S_{therm} = \xi_w C_{p,w} \ln T$ is the thermal entropy gained by ξ_w water molecules W_{III}.

The expressions for ΔH_{den} in Eq. (15) and for ΔS_{den} in Eq. (16) both repeat the paradigm of Class A of the hydrophobic hydration processes. By calculating enthalpy and entropy by Eq. (15) and Eq. (16), respectively, the total free energy change for cavity formation for the four compounds examined can be obtained. The curves present the expected shape (Fig. 8) with a maximum falling within the experimental range. The curves refer to the process of cavity formation and they can be used to calculate $\log K_{for}$ of cavity formation.

In order to give an answer to the objections of R. Lumry[9] and D.J. Winzor and C. M Jackson [11], we have considered here a sort of hydration equilibrium. In the protonation of carboxylic acids in aqueous solution, we have shown that not only the hydration reaction but also the actual combination of proton with the base contributes to the energetics of the reaction by a specific detectable protonation

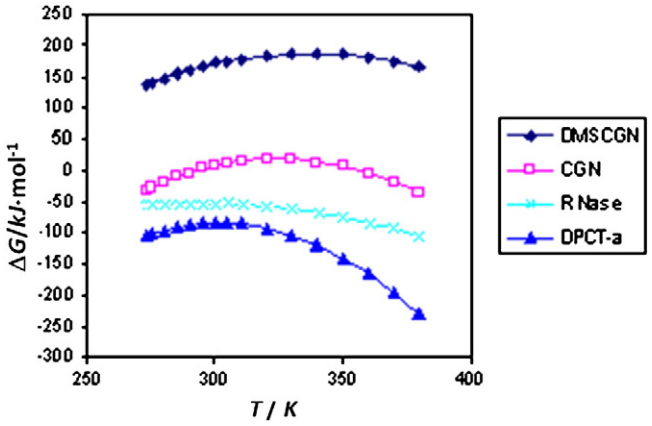

Fig. 8. Calculated free energies in protein denaturation.

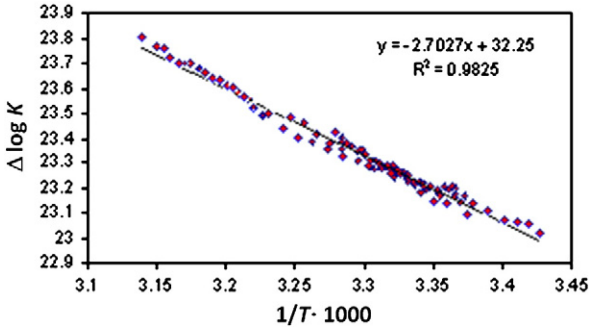

Fig. 9. van't Hoff plot of $\Delta \log K$ for RNase.

constant. We have, therefore, calculated the residual constant $\Delta \log K_x$ by calculating the difference between the constant $\log K_{den}$ of the experimental cumulative curve for each protein and the constant $\log K_{for}$ calculated by means of Eq. (15) and Eq. (16).

$$\log K_{den} = \log K_{for} + \Delta \log K_x \quad (17)$$

Then, $\Delta \log K_x$ has been plotted against $(1/T)$ thus obtaining linear van't Hoff plots (Fig. 9). The existence of linear plots $\Delta \log K_x = f(1/T)$ of the residual constant demonstrates that, coupled to the denaturation equilibrium between native and denatured form and to the dehydration reaction, there is also a protonation equilibrium that is active on three sites[3] at the very moment of denaturation.

Eq. (17) can be rewritten

$$\log K_{den} = \log K_{for} + \log K_{prot}. \quad (18)$$

From slope and intercept of the lines in the van't Hoff plot, the values of ΔH_{prot} and ΔS_{prot} have been calculated. The thermodynamic functions relative to each one-site reaction are obtained by deviding by three. All the values are reported in Table 5.

6. Thermodynamic functions by calorimetric determinations

The denaturation of proteins can be studied by calorimetry also. We can demonstrate that the enthalpy determined calorimetrically follows the same rules, as that found from equilibrium determinations.

The DSC microcalorimeter has been used by several Authors [15–19] to study the equilibrium between native and denatured conformations of macromolecules. The first set of data that we have analysed under the light of the FCB model is that reported by Privalov [16]. We have measured the peaks of the calorimetric traces obtained for HEW lysozyme under different pH and determined either by isothermal (IC) or differential scanning (DSC) calorimetry. The number of water molecules that we have calculated from the slope of the line is $\xi_w = 88.9$. Other sets of calorimetric data concerning various types of lysozyme have been obtained by J. M. Sturtevant and reported [20].

Typical plots of denaturation enthalpies against T_{den} for T4 lysozyme are presented in Fig. 10. Several different batches of proteins were used in each case and this could be the cause of the considerable scattering in the data. The temperature of denaturation T_{den} was varied by varying the pH over the range 1.8 to 3.1. The different mutants produce lines with different slopes corresponding to $\xi_w = 122$ for wild T4 lysozyme, $\xi_w = 131.4$ for Thr157Ala, and $\xi_w = 139.8$ for Arg96His, respectively.

The dehydration numbers obtained from thermal denaturation enthalpy for different types of lysozyme are reported in Table 6. The

[3] The factor 3 has been calculated from the displacements of the curves as the function of pH (cf. Table B.1)

Table 5
Thermodynamic functions calculated from the van't Hoff plot of Δlog *K* (*).

Protein	Equation	R^2	ΔH_{prot} kJ·mol^{-1}	$(1/3)\Delta H_{prot}$ kJ·mol^{-1}	ΔS_{prot} J·K^{-1}mol^{-1}	$(1/3)\Delta S_{prot}$ J·K^{-1}mol^{-1}
CGN	$Y = 3.0716(1/T) - 26.188$	0.9153	−51.41	−17.1	−120.3	−40.1
DMSCGN	$Y = 2.6851(1/T) - 6.2841$	0.9611	−58.81	−19.6	−501.4	−167.1
DCPT	$Y = -6187(1/T) - 19.764$	0.9156	+50.1	+16.7	−378.8	−126.2
RNase	$Y = -2.7027(1/T) + 32.25$	0.9825	+ 51.7	+27.2	+617.4	+205.8

(*) Division by 3 (cfr.power$\langle x \rangle = 3.04 \pm 0.08$ in Table B.1) to refer to a one-site reaction.

changes in the number of water molecules, ξ_w are coherent with the molecular features of the types of lysozyme. The variation between HEW and T4 lysozyme is related to the size of the molecules. The wild T4 lysozyme has a sequence of 164 residues against 126 of HEW lysozyme. The molecular weight of T4 Lysozyme is 18,700 Da against 14,100 Da for HEW lysozyme. On the whole, the molecule of T4 lysozyme is larger than the molecule of HEW lysozyme and very likely presents a number of hydrophobic residues which is roughly proportional to the molecular size. The changes of ξ_w between wild T4 lysozyme and its mutants are justified by the increased hydrophobic character of the substituents. Ala is more hydrophobic than Thr and His more hydrophobic than Arg, respectively

The values of the extrapolated enthalpy ΔH_{mot} obtained from calorimetry plotted against ξ_w yield values $\Delta h_{for} = -21.13$ kJ·mol^{-1}·ξ_w^{-1} and $\Delta H_0^{(\xi_w=0)}$ that are practically equal to those obtained by the van't Hoff equation (Table 7). They conform to the values obtained (with sign reversed) in micelle formation and protein folding, although they have been obtained in experiments of completely different types.

7. Calorimetric denaturation and cavity formation

In order to find a reasonable explanation of the mechanism of thermal denaturation, we presume that the folded native protein had been formed through a process of hydrophobic association analogous to that of micelle formation, with an outstanding positive entropic contribution. We recall that the hydrophobic bonding is driven by the positive entropy change, $\Delta S_{red} \gg 0$ produced as the consequence of the condensation of ξ_w water molecules W_{III} into water W_I, with cavity reduction $\mathbf{B}(\xi_w W_{III} + \xi_w W_{II} \rightarrow \xi_w W_I - \text{cavity})$. The folded native protein can be, therefore, assigned unitary values of the thermodynamic stepwise functions equal to those of the denaturation steps, with sign reversed. W_{III} is that part of the system that is giving rise to a change of phase, from structured to fluid state. When the heat supply starts, the heat moves a molecule of water W_{III} displacing the equilibrium toward the fluid state. The whole process (Table 8) takes place through three steps:

1) *Start*: the heat supplied to the system generates melting of some water W_{III}, creating the cavity. In fact, the creation of the cavity ($dV_{for} > 0$) produces negative entropy ($dS_{for} < 0$), thus beginning to cancel the positive entropic contribution of protein folding ($\Delta S_{red} + dS_{for}$).
2) *Scanning*: the process of heat supply continues (integration) until the total entropy change for cavity formation, $\Delta S_{for} \ll 0$ completely compensates for the entropy change $\Delta S_{red} \gg 0$ of the protein folding.
3) *Final:* at this stage ($\Delta S_{red} + \Delta S_{for} = 0$), the whole positive entropy contribution produced by folding is cancelled: the disruption of every hydrophobic bond is completed and the denatured state has become the stable one. The denaturation process, therefore, consists in the disruption, through cavity creation and negative

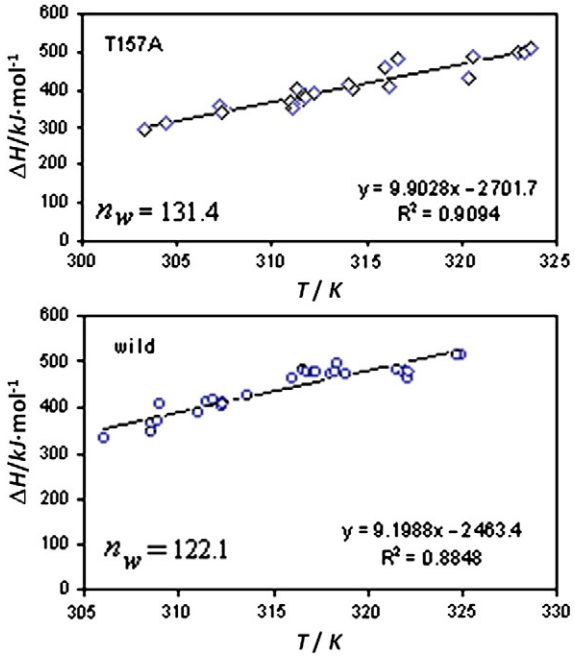

Fig. 10. Dependence of enthalpy on the temperature T_{den} for a wild type of lysozyme from bacteriophage T4 and its T157A mutant.

Table 6
Dehydration numbers, ξ_w from calorimetry in different types of lysozyme.

Type	Slope J·mol^{-1}K^{-1}	ξ_w	$\Delta H°$ kJ·mol^{-1}	T_{ad} (!) K
HEW	6701	88.9	−1764.8	263.4
wild T4	9199	122	−2463.4	267.8
T157A(T4)	9903	131. 4	−2701.7	272.8
R96H (T4)	10,539	139.8	−2896.2	274.8

(!)T_{ad} is the temperature where $\Delta H_{app} = 0$ (adiabatic).

Table 7
Enthalpy and entropy functions in corresponding processes(°).

Process	Class	$\Delta H_0^{(\xi_w=0)}$ kJ·mol^{-1}	Δh_w kJ·mol^{-1}·ξ_w^{-1}	$\Delta S_0^{(\xi_w=0)}$ J·K^{-1}·mol^{-1}	Δs_w J·K^{-1}·mol^{-1}·ξ_w^{-1}
Protein denat. (van't Hoff)	A	+211.82	−22.5	+415.8	−424.2
Protein denat. (calorim.)	A	+221.3	−22.6	–	–
Protein folding	B	−211.82	+22.5	−415.8	+ 424.2
Micelle formation	B	−3.97	+23.13	+ 10.2	+ 428
Non-polar gas solub.	A	−17.7	−21.6	−86.4	−445

(°) Δh_w and Δs_w indicate general unitary thermodynamic functions of either Class, i.e. Δh_w and Δs_w indicate Δh_{for} and Δs_{for}, respectively, in Class A and Δh_{red} and Δs_{red}, respectively, in Class B.

Table 8
Process of thermal denaturation.

Step	Exper.	Thermodynamic function	Physico-chemical process
0	Rest	$\Delta S_{red} = +\xi_w 424\ \mathrm{J\cdot K^{-1}\cdot mol^{-1}}$	*Native protein (folded)*
1	Heat supply start	$dQ/T = dS_{therm}$ $dS_{therm} \rightarrow dV_{for} > 0$ $dV_{for} \rightarrow dS_{for}$ $dS_{for} = -424\ \mathrm{J\cdot K^{-1}\cdot mol^{-1}}\, d\xi_w$ $\Delta S_{red} + dS_{for}$	W_{III} + *cavity formation* *initial break: hydrophobic bonds* *initial cancelling: entropy* ΔS_{red}
2	Scan	$\int_{T_1}^{T_2} C_{p,app} dT = Q_{cal}$ $Q_{cal} \rightarrow \int dS_{for} = \Delta S_{for}$ $\Delta S_{for} = -\xi_w 424\ \mathrm{J\cdot K^{-1}\cdot mol^{-1}}$	*Cavity: forming* *entropy* ΔS_{red}: *cancelling* *hydrophobic bonds: breaking*
3	Final	$\Delta S_{red} + \Delta S_{for} =$ $+\xi_w 424 - \xi_w 424 = 0$	*Entropy* ΔS_{red}: *cancelled* *hydrophobic bonds: broken* *protein: denatured (unfolded)*

entropy production of the entropy-driven hydrophobic bonds which had been keeping the chains folded.

The denaturation process can be represented also in a free-energy diagram (Fig. 11). We refer to the motive free energy of folding: a) (Fig. 11a) before heat supply starts, the folded native state is thermodynamically stable being, at any temperature, the motive (folding) free energy negative ($\Delta G_{fold} < 0$), due to the outstanding contribution of the positive entropy change ($\Delta S_{red} \gg 0$), b) (Fig. 11b) after completion of heat supply, the folding free energy has become positive because the negative entropy change ($\Delta S_{for} \ll 0$) due to cavity formation has completely cancelled the cavity reduction entropy gain at folding and hence the denaturation free energy is negative ($\Delta G_{unfold} < 0$).

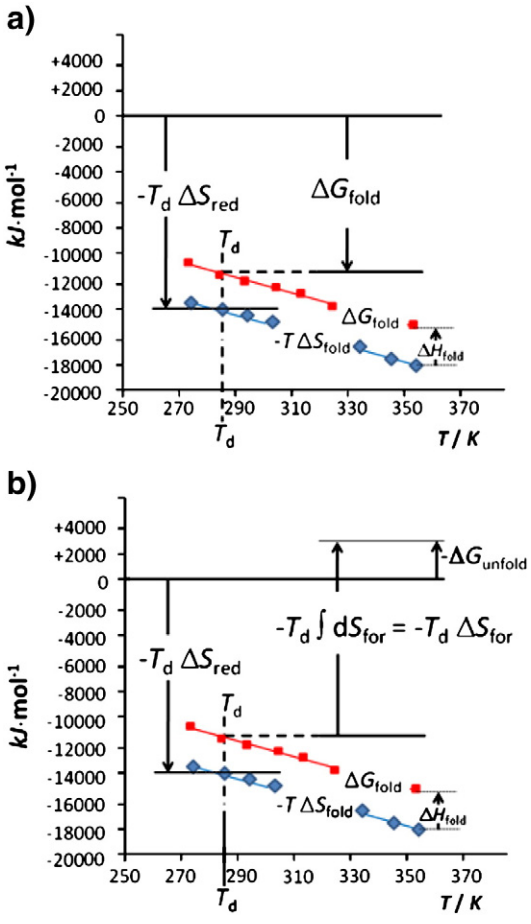

Fig. 11. a) Native folded state, stable ($\Delta G_{fold} < 0$) because entropy driven ($\Delta S_{red} \gg 0$). b) Thermal denaturation at temperature T_d : after heat supply, melting of water W_{III} has created a cavity, entropy consuming. $\Delta S_{for} \ll 0$ compensates for $\Delta S_{red} \gg 0$, leading to stable denatured state (unfolding) with $\Delta G_{unfold} < 0$.

8. Chemical denaturation and template effect

A proof of the constancy of slope ΔC_p, and hence of ξ_w, in the denaturation enthalpy of proteins has been shown by Pfeil and Privalov [15]. They report a diagram where denaturation enthalpy of lysozyme conforms to Eq. (3) with a constant slope either when the denaturation is obtained by thermal denaturation or by GuHCl denaturation (Fig. 12). This means that also by changing the concentration of denaturant we obtain the same parallel displacement of curves as that shown by Lumry [12] by changing $[H^+]$. This behaviour suggests that the reaction mechanism could be the same in either situation. We can suppose, therefore, that in chemical denaturation we are dealing with at least two coupled equilibria, the first one is the dissociation from the bulk of water W_{III} with creation of the cavity, with equilibrium between the three forms of water (W_I, W_{II}, and W_{III}) and the second process is the binding of ligand, like a proton or a denaturant.

The type of binding between protein and ligand could be direct or mediated through water. In the thermal denaturation of chymotrypsinogen we succeeded to demonstrate the existence of a protonation constant K_{prot} coupled to the hydration reaction constant K_{hydr}.

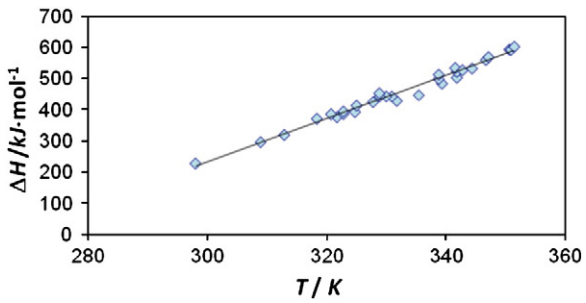

Fig. 12. a) Lysozyme. The slope is constant (i.e. ΔC_p is constant) whatever thermal or chemical denaturation and whatever the experimental method (data from Privalov [16]).

Table 9
Denaturants and stabilising molecules for proteins.

Denaturant	Stabilising
6 M GdnHCl	Sucrose
Urea	2-methyl-2,4-pentanediol (MPD)
2-Chloroethanol 40%	Glycine–betaine
Methoxyethanol 40%	Na_2SO_4
	Glycerol
	Trimethylamine-N-oxide (TMAO)

S. N. Timasheff, et al. [21] have studied the role of solvation in protein stabilisation and unfolding believing correctly that the problem of chemical denaturation is strictly connected to the opposite process of stabilisation. The types of denaturing and stabilising molecules are apparently different (Table 9). According to these authors, all denaturants examined (urea, guanidinium hydrochloride, 2-chloroethanol, methoxyethanol) should interact preferentially with proteins. Urea and guanidinium hydrochloride are supposed to interact with peptide groups, while the alcohols should interact with the non-polar residue, relieving the hydrophobic pressure of water and permitting the structure to loosen. In regard to stabilisation, Timasheff et al. observe that stabilising agents are polyhydric compound containing solvents such as aqueous glycerol, sucrose, and hexylene glycol, (2-methyl-2,4-pentanediol (MPD)). Lee and Timasheff [22] have analysed the interactions with solvent components of proteins in guanidinium hydrochloride and propose an interaction between protein and denaturant mediated by an intimate contact between denaturants and portions of the protein molecule. Timasheff [23] finds, however, that the binding affinity of the chemical denaturants urea or GuHCl is rather low, similar to hydration affinity, and in fact the denaturant would be in competition with water for the same binding sites. In contrast, Poland [24], by examining the effect of GuHCl on the denaturation of ferro- and ferri-cytocrome C, concludes that free energy depends on changes of log$c$ (c = [GuHCl]). He calculates two equilibrium constants, $K(II) = 4.305 \cdot 10^{-8}$ for Fe(II) protein and $K(III) = 1.079 \cdot 10^{-3}$ for Fe(III) protein. This means that GuHCl behaves, at least in this case, as a ligand forming a strong bond with the protein.

By considering that a direct protein–denaturant interaction might be responsible of the denaturing action we have analysed the data reported by Timasheff et al.[21]. The analysis, however, has shown that in any case the affinity between protein and denaturant is very low and not sufficient to cancel the favourable entropy-driven affinity of folding. The interactions between protein and denaturant are not so strong to displace the denaturation equilibrium to the field where the denatured state is thermodynamically stable. J. A. Schellman [25] had arrived at the same conclusion that the interaction of urea with a protein site is extremely weak.

J. A. Schellman has analysed also the importance of the excluded volume effect in denaturation. He observes that in weak binding of denaturant to protein, the second virial coefficient is negative, thus showing a parallelism with cavity reduction of the FCB model. In this contest it is worth noting that both the expansion of polypeptide chains in denaturants [26] (we recall cavity formation in Class A of FCB model) and their contraction in stabilising osmolites [27] (we recall cavity reduction in Class B of FCB model) have been observed experimentally.

We can consider, at this point, that the direct binding, similar to that observed in protonation, might not always be necessary for denaturation. We can suppose that the action of the denaturant is analogous to that exerted by heat supply in thermal denaturation. The action of the denaturant (urea or guanidinium) on the equilibrium **A** ($-\xi_w W_I \rightarrow \xi_w W_{II} + \xi_w W_{III}$ + cavity) is toward the formation of the cavity, by binding preferentially to molecules of water W_{II}, thus producing negative entropy for cavity formation. (Fig. 13). This negative entropy compensates for the positive entropy gain produced

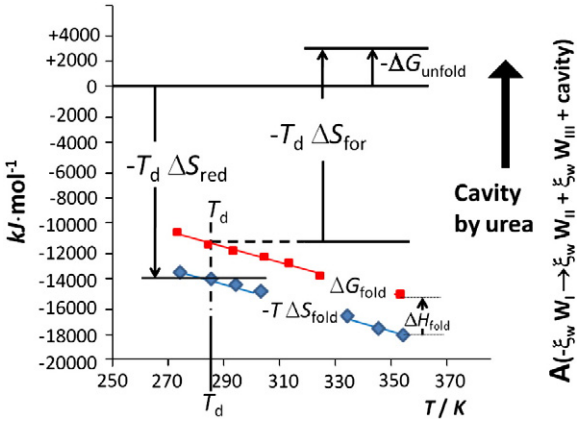

Fig. 13. The action of denaturant displaces the equilibrium in water toward formation of cavity with negative entropy production, that cancels the positive entropy gain of folding.

by folding and brings the protein toward the level where the denatured protein is stable. This behaviour of denaturant not dependent from direct urea/protein affinity, explains the denaturing action of other polar substances such as 2-Chloroethanol 40% or Methoxyethanol 40% that look suited to modulate, with their linear shape, the equilibrium between the various forms of water W_I, W_{II}, and W_{III} toward W_{II} and cavity formation. We can speak of "*template effect*" on water structure. The stabilising agents, in contrast, should be structurally suited to modulate the equilibrium between the forms of water toward the preferential formation of water W_I, that presents a

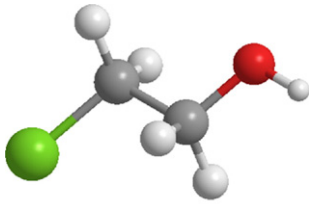

2-Chloroethanol

tetrahedral structure, roughly speaking. This could explain in particular the stabilising action of TMAO [28]. By adding TMAO, the Bolen group was able to refold an altered form of ribonuclease that *per se* was unable to fold in a stable conformation. Another stabiliser is MPD, whose structure can be schematically represented by two tetrahedra joined by a common apex. K. Anand, D. Pal and R. Hilgenfeld [29] have analysed crystal structures of complexes formed by proteins with MPD.

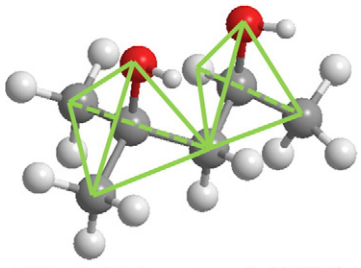

2-Methyl-2,4-pentanediol (MPD)

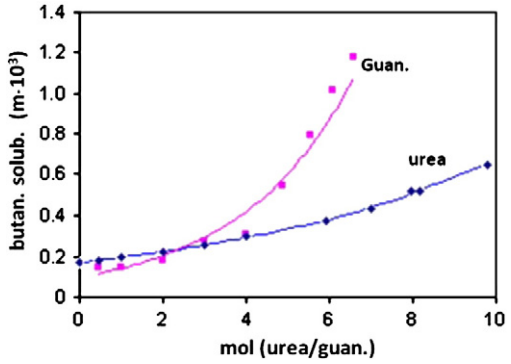

Fig. 14. Solubility of butane in aqueous solutions of urea and of guanidinium hydrochloride.

These authors suggest that MPD promotes stabilisation of the protein by preferential hydration, which is facilitated by attachment of MPD molecules to the hydrophobic surface. Translated into the terminology of the FCB model this would mean a template effect for stabilisation of water W_I with cavity reduction.

The *template effect* of denaturants favouring water W_{II} and that of stabilisers favouring water W_I parallels the distinction between *chaotropic* substances (denaturants, structure breaking) and *kosmotropic* (stabilisers, structure making) [30,31]. This dramatically biblical terminology looks rather out of place for a phenomenon that perhaps is only a question of a templating preference for water W_I rather than W_{II} or *vice versa*, with minimal differences in energy.

The weakness of the interaction between water and denaturant is in agreement with the action of various denaturants on folding/unfolding transitions. For example, when concentrated guanidinium hydrochloride is diluted out of a sample of chemically denatured hen lysozyme, the protein refolds, spontaneously. In other words, the folded state (cf. Fig. 11a) is energetically favoured in the absence or scarcity of chemical denaturant. Therefore, when guanidinium concentration is low, the equilibrium between the different forms of water is no longer displaced toward cavity formation and the protein goes back to the folded state.

9. Salting-out and salting-in

There is also a correspondence between stabilisers and salting out substances like ammonium sulphate, $(NH_4)_2SO_4$. This substance decreases the solubility of proteins and is employed to facilitate precipitation of the proteins. Ammonium sulphate gives origin in aqueous solution to two tetrahedral ammonium ions and one tetrahedral sulphate anion that are good templates for W_I and cavity reduction, similarly to the elements of Class B of the FCB model. This behaviour indicates definitely that the salting-out effect is a member of Class B in the realm of the hydrophobic hydration processes.

On the other hand, there is correspondence between denaturants and salting-in substances, like potassium thiocyanate, KSCN, that increase the solubility of non-polar substances.

Thiocyanate gives origin to a linear anion SCN^- that works as template for W_{II} and cavity formation, similarly to the elements of Class A of the FCB model. Other very good templates for W_{II} and cavity formation are urea and GuHCl. A larger cavity facilitates acceptance of more solute molecules and hence an increase of the solubility. This behaviour is indicative that the salting-in effect is a hydrophobic hydration process belonging to Class A with cavity formation.

The salting-out effect is difficult to evaluate quantitatively but salting-in can be evaluated, by measuring the increase of solubility. Wetlaufer et al. [32] have studied the solubility of butane in urea solutions and in guanidium chloride solutions. Their results give us the chance to evaluate the validity of the hypothesis on the kind of templating action of these denaturants. On the basis of the FCB model, the inspiring idea is that urea (or guanidinium) coupled to the reaction $\mathbf{A}(-\xi_w W_I \rightarrow \xi_w W_{II} + \xi_w W_{III} + \text{cavity})$, tends to associate to W_{II}, thus displacing the reaction toward the formation of the cavity. The solubilities of butane follow exponential curves: the curve for guanidinium hydrochloride is about three times steeper than that for urea (Fig. 14). Actually, we can observe (Fig. 15) that on the basis of the molecular structures, the possibilities of binding of water via hydrogen bonds NH…O to GuHCl (B) are more than those of urea (A). Therefore, guanidinium hydrochloride is about three times more efficient than urea in templating for solvent molecules W_{II} and cavity formation.

The solubilities of butane in urea and in GuHCl, reported as the function of ln[Denaturant] give the following expressions:

$$\text{urea}, c_{butan} = -1.78 + 0.139\ln[\text{urea}] \left(R^2 = 0.9991\right)$$

$$\text{GuHCl}, c_{butan} = -2.54 + 0.398\ln[\text{GuHCl}] \left(R^2 = 0.9769\right).$$

At the moment, the exact thermodynamic relationship connecting denaturant concentration to solubility of hydrocarbon is not clear. Probably, the thermodynamic relation depends on the type of reaction coupled to the reaction of cavity formation. It is evident, however, that the better efficiency of GuHCl rather than urea can be evaluated by the

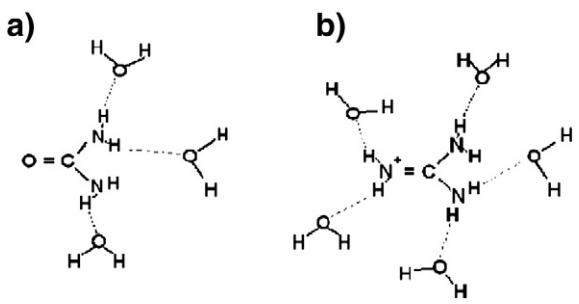

Fig. 15. Hydrogen bonding of water to urea (A) is less efficient than to guanidinium ion (B). Salting-in effect is lower in urea solutions than in guanidinium solutions.

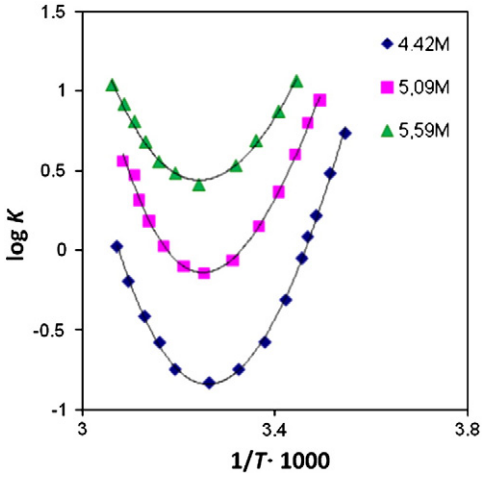

Fig. 16. β-globuline: the curvatures are decreasing at high concentration of urea, i.e. ΔC_p is sharply decreasing when urea concentration is large enough (from Ref. [34]).

Table 10
Denaturation of β-lactoglobuline. Change of number ξ_w at high urea concentration.

Urea conc.	4.42 M	5.09 M	5.59 M
ξ_w	118.2	117.7	92.1
$\Delta\xi_w$	–	−0.47	−25.6

Table 11
Curvatures (ξ_w) of hydrocarbons solubility in water, and in concentrated urea solution.

Compound	Water	Urea 4 M
	ξ_w	ξ_w
Methane	2.6	0.47
Ethane	3.5	1.22
Buthane	4.72	3.54

power of concentration, $[GuHCl]^{0.398}$ with respect to $[urea]^{0.139}$, with a ratio 0.398/0.139 = 2.864 clearly dependent on the better ability of forming hydrogen bonds with W_{II}.

Other effect of salting-in can be found in the changes of denaturation free energy by addition of denaturant. According to Haynie [33], the action of denaturant on free energy is represented by

$$\Delta G_{den} = \Delta G_{den}^{\circ} - mc \tag{19}$$

where ΔG_{den}° is the free energy in the absence of denaturant, c is the denaturant concentration and m is a parameter that depends on temperature, pH, and, of course, the protein. In some cases, however, the dependence on denaturant concentration is decisively non linear.

These uncertainties in the type of dependence upon denaturation concentration, reflect the variety of possible reactions coupled to the reaction $\mathbf{A}(-\xi_w W_I \rightarrow \xi_w W_{II} + \xi_w W_{III} + \text{cavity})$ of cavity formation.

10. Excess urea

If the number ξ_w of molecules W_{III} is constant, the curvature of the plot $\log Q_{den} = f(1/T)$ remains constant at the variation of denaturant concentration, similarly to the plots of Fig. 3. Creation of water W_{II} is accompanied by formation of a cavity, thus facilitating the insertion of the hydrocarbon chains of the denaturing protein in the solution. The constancy of ξ_w, however, is apparently not always maintained when the denaturation concentration is high enough, as shown by Pace and Tanford [34] for β-lactoglobuline. In fact, if we plot $\log K_{den}$ vs. $(1/T)$ for β-lactoglobuline at high concentration of urea, the curvature begins to decrease (Fig. 16). If we calculate the tangent to these curves at different temperatures and plot the tangents (i.e. ΔH_{den}) against the temperature T, we obtain values of ξ_w that are changing with the concentration of urea. The variation $\Delta\xi_w$ is (Table 10) almost null from 4.42 M urea to 5.09 M urea (ξ_w changes from 118.2 to 117.7 with $\Delta\xi_w = 0.5$), thus indicating that it is just at the end of constant ξ_w regime but becomes appreciable by passing from 5.09 M to 5.59 M (ξ_w changes from 117.7 to 92.1 with $\Delta\xi_w = 25.6$). The slope of the line

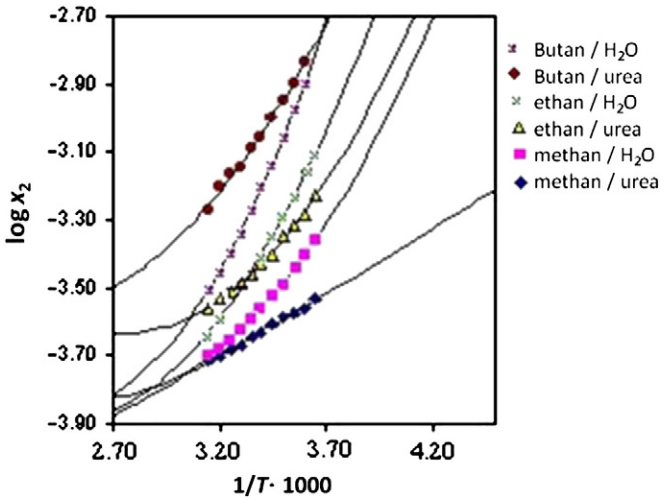

Fig. 17. Solubility of hydrocarbons in water and urea at different temperatures.

depends, according to the FCB model, on the number ξ_w of water molecules W_{III}, experimentally determined by *TED*, set free to form a cavity to host the unfolded branches of the macromolecule. Because we do not think that a lower value of the number ξ_w could indicate a smaller cavity to host the same branches, we must conclude that the only explanation possible for the action of urea according to the FCB model, is that urea itself promotes formation of W_{II} and melting of W_{III}. The molecules of denaturant in excess, however, at the higher concentrations begin to combine with the water molecules W_{III} set free by the reaction $\mathbf{A}(-\xi_w W_I \rightarrow \xi_w W_{II} + \xi_w W_{III} + \text{cavity})$. In such a way, the number ξ_w of free water W_{III} experimentally detected seems to correspond to a smaller cavity, what really is not the case. In fact, one part of the molecules W_{III} expelled from the cavity, has been sequestered by the excess of denaturant and is no longer free and cannot be detected as such by *TED*

The binding of denaturant in excess to water W_{III} has been confirmed by analysing the solubility of hydrocarbons in water and in urea solutions at different temperatures as determined by Wetlaufer et al. [32]. The curvatures of the solubility in water (Fig. 17) are higher than those in concentrated urea. This shows that in urea solutions the number ξ_w is smaller than in water (Table 11), because in these cases again one fraction of water W_{III} expelled from the cavity is absorbed by urea in excess and cannot be detected as free by means of *TED*.

11. Comparisons with molecular calculations

The conclusions of the FCB model can be compared with the results of molecular calculations that have been applied in many cases to the hydrophobic processes.

F. Vanzi, B. Madan, K.Sharp [35] have analysed the effect of the protein denaturants urea and guanidinium on the water structure. Changes in the hydrogen bond's network of water in the first hydration shell were analysed in terms of the random network model (RNM) using Monte Carlo simulations. According to their results, bulk water consists of two populations of hydrogen bonds: a predominantly linear population and a small but significant population of slightly longer and more bent hydrogen bonds. In a previous work [36] K.A. Sharp and B. Madam had shown that it is possible to distinguish two hydrogen bond populations: a larger population with quasi tetrahedral ice-like population with $\theta_h \approx 12°$ and a smaller population in which a fifth molecule, a mismatch water comes into the coordination shell of the central water molecule, forming a highly distorted H-bond with $\theta_h \approx 52°$. We can identify the former population with water W_{II} and the latter population with water W_I. They have also found that non polar solutes (comparable to Class A of the FCB model) tend to decrease the second population by competing for the position of the mismatch water molecule. Polar solutes, however, have the opposite effect, comparable to Class B of the FCB model. They recall two of the possible binding mechanisms put forward by Wetlaufer et al. [32]: one mechanism postulated for the denaturing activity of urea and guanidinium involves binding to protein groups exposed to solvent. Another possible mechanism is through effect on water structure, and thus on the strength of the hydrophobic effect. They state, however, that demonstrating that this mechanism, rather than direct binding to protein groups, is sufficient to denature proteins has proved to be elusive. A necessary condition for the direct effect on water structure should be, according to Sharp and Madam, that these denaturants

affect the structural and thermodynamic properties of water in a unique way (unique in the sense that distinguishes them from the effect on water of solutes that are *nondenaturing*).

Particularly they underline the fact that the hydrogen bond angle between waters in the first hydration shell, is a powerful way to analyse solute-induced perturbations for two reasons: (1) It is sensitive to structural perturbations, (2) The structural changes may be directly and quantitatively related to a key thermodynamic property, the heat capacity ΔC_p. Ample experimental data (we can recall our Eq. (1) and comments thereafter) have shown that hydration heat capacity change is the most revealing of the common thermodynamic functions (the others being free energy, enthalpy, and entropy) in terms of the differences between hydration of polar and non-polar (hydrophobic) solutes.

From this point on, however, the correspondence with the FCB model is failing. In fact, according to our calculations, heat capacity ($\Delta C_p = \xi_w C_{p,w}$) is bound to the reaction of water W_{III} whose stoichiometric coefficient ξ_w has been determined by us making use of *TED*. In the absence of the essential component W_{III}, the model of Sharp and Madam cannot explain the formation of cavity and the related relevant entropy change. The origin also of thermal enthalpy, ΔH_{therm} and thermal entropy, ΔS_{therm} and their strict interrelationship ($\Delta S_{therm} = \Delta H_{therm}/T$) cannot be explained, and many other properties of the systems, as well.

According to the calculations of Widom, Bhimalapuram, and Koga [37], the hydrophobic effect both as a cause of low solubility and of hydrophobic bonding, can be satisfactorily explained by referring to an Ising lattice model in Bethe–Guggenhheim approximation. Alternatively the same approximation they obtain by Montecarlo calculations. Both methods reach the conclusion that hydrophobicity is temperature dependent, in agreement with the conviction that the hydrophobicity effect becomes stronger with increasing temperature. These conclusions are clearly in contrast with our findings that the effect of the temperature on hydrophobic solubility and hydrophobic bond is due exclusively to the transformation undergone by water W_{III} (ΔS_{therm} and ΔH_{therm}). The actual hydrophobic repulsion (Class A) is independent from the temperature and is ruled by the negative entropy change ($\Delta S_{for} \ll 0$) associated to cavity formation. The hydrophobic attraction or hydrophobic bond (Class B) is again independent from the temperature and ruled by the positive entropy change ($\Delta S_{red} \gg 0$) associated to cavity reduction. Therefore also the model of Widom, Bhimalapuram, and Kohas has to be considered as inadequate to explain the hydrophobic effects.

P. J. Rossky [38] thinks that some of the earlier discussions on the mechanism of unfolding by urea focused on perturbation of water structure per se (Frank and Franks [6]), the so-called "indirect" mechanism has not received much support from experimental or simulation studies of aqueous urea. The alternative "direct" mechanism, implying a causative interaction between urea and the polypeptide, has been clearly evidenced, according to P. J. Rossky, in the simulated pathways. This point of view of Rossky is clearly in contrast with the conclusions of our work.

These are not the only discrepancies between the FCB model and the theoretical models proposed in the literature. In fact, a surprising feature of the unitary thermodynamic functions calculated by us for the various steps of all the hydrophobic processes ($<\Delta h_{for}>_A = -22.2 \pm 0.7$ kJ·mol^{-1}·ξ_w^{-1}, and $<\Delta s_{for}>_A = -445 \pm \Delta$ J·K^{-1}·mol^{-1}·ξ_w^{-1} in Class A, and $<\Delta h_{red}>_B = +23.7 \pm 0.6$ kJ·mol^{-1}·ξ_w^{-1}, and $<\Delta s_{red}>_B = +432 \pm \Delta$ J·K^{-1}·mol^{-1}·ξ_w^{-1} in Class B) is that they have been calculated by including results obtained from both large and small molecules. This indicates that the same type of unitary reaction is taking place in every case, independently from the total size of the reactant. This result is very important because it is in contrast with some theories supported by molecular calculations [39,40]. According to Chandler [39], there should be a cross-over point of behaviour by the solvent, passing from small to large solutes. The solute of small size should accommodate within the interstices of the structure of water, whereas, beyond a certain length-scale of the molecule, a type of molecular hydrophobic interface in the solvent should become thermodynamically and energetically feasible. In the former case the hydrophobic effect would be proportional to the volume of the small solute, whereas in the latter the effect would be proportional to the surface of the large solute molecule. The passage from one to another type of reaction would take place at a specific cross-over point that can be calculated by an appropriate algorithm. Actually, according to the FCB model, the type of reaction in the solvent is the same both in small and large molecules: it is the transformation **A** ($-\xi_w W_I \rightarrow \xi_w W_{II} + \xi_w W_{III}$ + cavity).

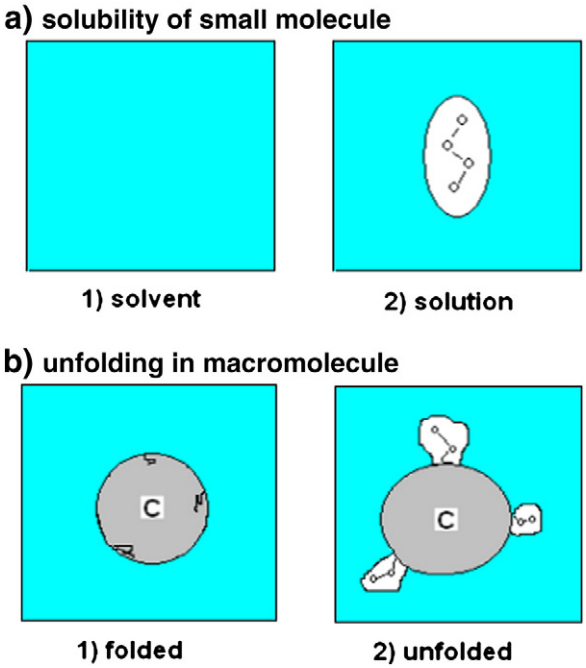

Fig. 18. a) Small molecule: the cavity surrounds the whole molecule; the trapped gas molecules lose their configurational entropy ($\Delta S_0^{(\xi w=0)} = -86.4$ J·K^{-1}·mol^{-1}). b) Macromolecule: the cavity surrounds only the unfolded chains; the core C remains almost invariant but the solvent volume is reduced and the solute becomes more concentrated ($\Delta S_0^{(\xi w=0)} = -59.7$ J·K^{-1}·mol^{-1}).

The point of view of Chandler is reinforced by S. Rajamani, et al. [40] who write that as the solute size is increased, water dewets the solute surface. Near a sufficiently large solute, the solute–solvent interface should resemble that between vapour and liquid water, and therefore should require interfacial thermodynamics for its recognition. Correspondingly, the thermodynamics of hydration should change gradually from entropic for small solutes to enthalpic for large solutes. The theoretical approach by Lum et al. [41] provided a quantitative description of structural and thermodynamic aspects of hydrophobic hydration over the entire small-to-large length scale region.

Yamirsky and Vogler [42] share this point of view that there is a gradual passage from small to large scale because they organise their article around length scale as a means of resolving commonalities between seemingly disparate phenomena that are all outcomes of hydrophobic hydration. Their major section is concerned with hydrophobic (dissolution) of small hydrophobic molecules such as methane and extends this discussion to self assembly or aggregation of hydrophobic molecules in a manner consistent with what has become a traditional bifurcation of hydrophobic effects into two categories: (i) hydrophobic hydration, and (ii) hydrophobic bonding. These authors, however, are sceptical about the possibility that theoretical simulations of the behaviour of too few molecules near hydrophobic interloper are suitable to reveal an alteration in vicinal water density brought about by a collective change in self association. At the same time, they are dubious about the capacity of a thermo-

chemical experiment involving too many water molecules to reveal the averaging behaviour of the relatively few water molecules in direct contact with a hydrophobic entity. After such uncertain statements, there is little wonder how the hydrophobic hydration literature has become so entangled.

The contradictions of these statements with the conclusions of the FCB model are apparent. The antinomy large/small scale, however, is resolved if we keep that the denaturation is characterised by the creation of a cavity in the solvent to allocate only the unfolded chains of the macromolecule, in the same way as this occurs, for the entire molecule, with small compounds (Fig. 18). It is sufficient to admit that in large molecules, the number of unfolding chains is proportional to the surface of the macromolecule, what is reasonable, and the contradiction disappears.

We should reject, however, the idea that a certain type of molecular hydrophobic interface in the solvent, typical of large scale molecules might become thermodynamically and energetically feasible. This misunderstanding on the structure of the solvent has been probably born by the fact that a change of mechanism exists on the side of the solute. In fact, with small molecules, we are dealing with a solubilisation process from gas to solution whereby the whole molecule needs a cavity large enough to surround the whole molecule. According to the FCB model, the solubility reaction, that belongs to Class A, can be subdivided in successive steps. The first step consists of the passage of the molecules from the disordered gaseous state to the condensed state trapped in the cavity of the solvent. Associated to this step,[4] there is an extrapolated (cf. Eq. (12)) entropy change $\Delta S_0^{(\xi w=0)} = -86.4\ \mathrm{J\cdot K^{-1}\cdot mol^{-1}}$, that measures the loss of configurational entropy by the trapped molecules. It is worth noting that in the solubility of liquids the same step entropy[5] is practically null ($\Delta S_0^{(\xi w=0))} = -0.5\ \mathrm{J\cdot K^{-1}\cdot mol^{-1}}$). The lack of entropy loss in the liquids is in accordance with the absence of translational entropy. In fact, the liquids, before being dissolved, are already condensed. For macromolecules we can consider as process of Class A the denaturation reaction. The process of unfolding involves only the hydrophobic chains of the external surface. Each chain needs a cavity proportional to its own volume only, to be allocated. The core of the macromolecule, instead, constitutes a volume excluded to the solvent both before and after unfolding. In regard to the process of folding/unfolding the core volume undergoes minor changes. The corresponding negative step entropy in the group of proteins examined is $\Delta S_0^{(\xi w=0)} = -59.7\ \mathrm{J\cdot K^{-1}\cdot mol^{-1}}$ (cf. Table 3) and is probably due to an increase of the concentration of the solute caused by the sum of the cavities allocating the unfolded chains. The sum of cavities represents, in fact, further volume excluded to the solvent.

All these notes about the specificities of the extrapolated entropy in different families of reactions of Class A demonstrate unequivocally that it is in the properties of the solute that we can find discontinuities or cross-over points, but not in the behaviour of the solvent. It is clear that on the side of the solvent, the only and the same type of reaction $\mathbf{A}(-\xi_w W_I \rightarrow \xi_w W_{II} + \xi_w W_{III} + \text{cavity})$ has taken place, both in small and large molecules.

The problem of the bifurcation of hydrophobic effects into two categories is brilliantly resolved in the FCB model by the subdivision of the hydrophobic hydration processes into the two classes A and B, with their types of reactions, direct or inverse, respectively. At the same time, the effect of few molecules ξ_w W_{III} contributing exclusively to both thermal enthalpy and thermal entropy is suitable to reveal, by thermodynamic experiments based on *TED*, the changes with temperature of the thermodynamic functions. These few water molecules W_{III}, in thermal denaturation, become, through their passage of state from structure to fluid or vice versa, the key to open the zip fastener formed by the entropy-driven hydrophobic bonds that had been keeping the chains folded in the native state.

Other authors, however, have put forward ideas conforming more or less with the FCB model. H. S. Frank and M. W. Evans [43] and G. Nemethy and H. A. Scheraga [44] suggested that water is caging around non-polar gases, a distorted structure enabling the maintenance of hydrogen bonds that water cannot form with the hydrophobic core. In the process of this rearrangement, enthalpy is gained (cf. $\Delta H_{for} = -\xi_w \cdot 22.5\ \mathrm{kJ\cdot mol^{-1}}$, with unitary enthalpy change $\Delta h_{for} = -22.5\ \mathrm{kJ\cdot mol^{-1}\cdot \xi_w^{-1}}$) at the expense of entropy loss (cf. $\Delta S_{for} = -424.2\ \xi_w \mathrm{J\cdot K^{-1}\cdot mol^{-1}}$, with unitary entropy change $\Delta s_{for} = -424.2\ \mathrm{J\cdot K^{-1}\cdot mol^{-1}\cdot \xi_w^{-1}}$). The point concerning entropy loss for cavity formation is accepted by Graziano [45] who asserts, however, that insertion of a solute molecule in a liquid phase significantly restricts the configurational space accessible to solvent molecules, providing a large and negative entropy change This assertion by Graziano is in contrast with the FCB model, that considers that the configuration entropy loss $\Delta S_{for} \ll 0$ is referred to the solute that is now more concentrated in a smaller volume, whereas ξ_w water molecules W_{III} expelled from the solvent to form the cavity (i.e. the excluded volume effect) acquire the thermal entropy $\Delta S_{therm} = \xi_w C_{pw} \cdot \ln T > 0$. H. Frank and F. Franks [6] have proposed a mechanism of unfolding focused on perturbation of water structure by urea, a mechanism that is similar to that proposed by us in the present model. Y. D. Livney, R. Edelman, I. Kusner, R. Kisiliak, S. Srebnik [46] have combined mathematical modelling and laboratory experiments to study the stereochemical structure effect on hydration of three isomeric aldohexoses: glucose, galactose, and mannose. The atomistic simulation was developed and used to quantify the compatibility of each aldohexose molecule with ideal tetrahedral water structure as embodied in hexagonal ice. These results support the template concept, proposed by the FCB model, as the basis to explain the stabilising effect of these substances on the water structure W_I.

12. Conclusions

The analysis of free energies, enthalpies, entropies of protein denaturation has shown that the model proposed for the hydrophobic hydration processes is suitable to explain the thermodynamic changes occurring in protein denaturation. Application of the *TED* principle has made possible the determination of the number ξ_w of water molecules W_{III} involved in each denaturation process. The ξ_w water molecules W_{III}, ($\xi_w > 0$) released in the denaturation process correspond to the formation of a cavity to host the unfolding branches of the macromolecule. The molecular mechanism of cavity formation in the solvent structure is the same as that in inert gas solubilisation. The change of phase of ξ_w water molecules W_{III}, expelled to form the cavity, is the only reaction that generates the high value of the isobaric heat capacity ΔC_p at denaturation and consequently these water molecules are the only contributors to the thermal enthalpy, $\Delta H_{therm} = T\Delta C_p$ and to the thermal entropy, $\Delta S_{therm} = \ln T\, \Delta C_p$. The decisive role of these water molecules with their change of phase in the denaturation process has to be stressed upon. Coupled to this process of melting, other processes of cavity formation and of protonation are active at denaturation. This demonstrates that, notwithstanding the doubts raised by Winzor and Jackson [11], it is possible to arrive at a complete thermodynamic description of protein interactions.

We can recall that in the folding of proteins, in contrast to denaturation, the number $-\xi_w$ of water molecules W_{III} corresponds to a process of cavity reduction with production of positive entropy and formation of hydrophobic bonds, the same process that takes place in micelle formation. The thermal denaturation consists, therefore, of the gradual disruption by the heat supplied, via the

[4] cf. Ref. [4], paragr. 6.1, p. 124.
[5] cf. Ref. [4], paragr. 6.2, p. 126.

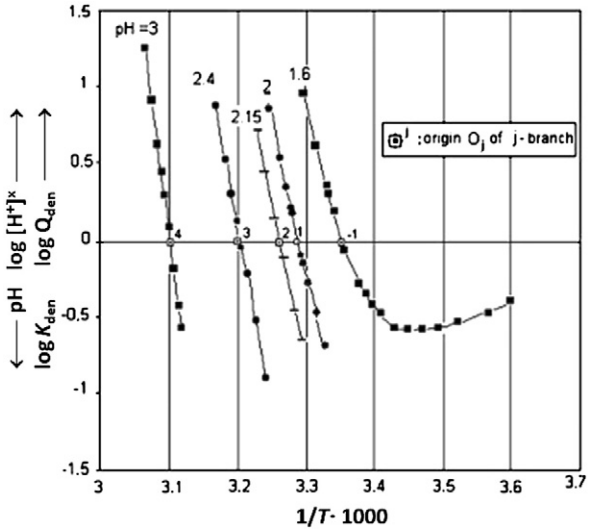

Fig. B.1. Determination of denaturation free energy at different pH. and different temperatures. The curve at each pH is the branch br_j(pH = 3, or 2.4,…) with origin at O_j.

production of negative entropy for cavity formation, of the entropy-driven hydrophobic bonds that had been keeping the chains folded. The action of chemical denaturants like urea, guanidinium chloride or others is similar to that exerted by heat. The denaturant displaces the equilibrium $\mathbf{A}(-\xi_w W_I \rightarrow \xi_w W_{II} + \xi_w W_{III} + \text{cavity})$ toward the formation of the cavity, with production of negative entropy. By considering that the stabilising substances affect this equilibrium in the opposite way favouring the formation of water W_I, this proves that these denaturants affect the structural and thermodynamic properties of water in a unique way (unique in the sense that distinguishes them from the effect on water of solutes that are *nondenaturing*), as required by Sharp and Madam [36]. The comparison of the specific characteristics of the present model with the result of the many molecular calculations has revealed that some points of agreement exist, mainly in the simulations of Sharp and Madam [36]. Two decisive features, however, are in contrast with the FCB model: (i) the separation between thermal and motive components of the thermodynamic functions is not taken into account in the molecular calculations, thus ignoring the specific behaviour of water W_{III}, associated to the thermal components, as well as the process of cavity formation, associated to the motive components; (ii) the cross-over point described by the molecular calculations for the

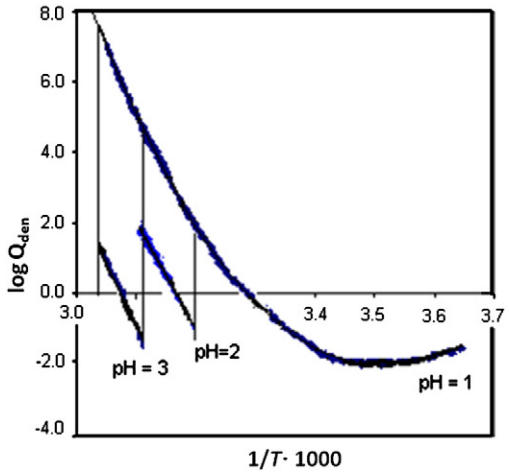

Fig. B.2. Sections of the cumulative denaturation curve can be moved to the range of log Q around 0 by increasing pH. The shape of the curve is invariant because ΔC_p is constant.

behaviour of the solvent when passing from small to large molecules of solute is absolutely excluded by the FCB model.

The separate enthalpy and entropy terms attributable to the different steps of the hydrophobic hydration processes are numerically very close to each other, respectively, in the different processes and the results of the present research on denaturation confirm those findings.

Acknowledgements

This work was supported by the contributions from the Cassa di Risparmio di Parma Foundation and the University of Parma.

Professor G.P. Chiusoli, Emeritus, University of Parma, is warmly thanked for assistance in the presentation of the paper.

Appendix A. Denaturation equilibria and thermodynamic functions

The equilibrium between native *N* and denatured *D* state of a protein can be decomposed into two steps. The first process is the conformational transition from the *D* to *N* state with the constant Q_{conf}

$$Q_{conf} = [\mathrm{D}] / [\mathrm{N}] \tag{A.1}$$

The second process is the hydration of the denatured state via the formation of a cavity in the bulk of the solvent molecules by expulsion of water molecules W_{III}

$$\mathrm{D} + x\mathrm{W} = \mathrm{D}_w + \xi_w \mathrm{W}_{III} \tag{A.2}$$

with equilibrium constant

$$K_{hydr} = [\mathrm{D}_w] \times \left[(\mathrm{W}_{III})_T\right]^{\xi_w} / [\mathrm{D}] \tag{A.3}$$

where $[\mathrm{D}_w]) \gg [\mathrm{D}]$ is the concentration of hydrated denatured molecules, $[(W_{III})_T]$ is the activity,[6] temperature dependent, of water molecules W_{III}, and ξ_w is the number of water molecules expelled from the bulk to form a cavity. By substitution of Eq. (A.1) into Eq. (A.3) we obtain

$$K_{hydr} Q_{conf} = [\mathrm{D}_w] \times \left[(\mathrm{W}_{III})_T\right]^{\xi_w} / [\mathrm{N}] = K_0 \tag{A.4}$$

The denaturation quotient is (cf. Eq. (B.4))

$$Q_{den} = [\mathrm{D}_w] / [\mathrm{N}] \tag{A.5}$$

and then by introducing Eq. (A.3) and Eq. (A.4) into Eq. (A.5), we obtain

$$Q_{den} = K_0 \times \left[(\mathrm{W}_{III})_T\right]^{\xi_w}. \tag{A.6}$$

By taking the logarithms and multiplying by *R*, we obtain

$$R\ln Q_{den} = R\ln K_0 - \xi_w R \ln\left[(\mathrm{W}_{III})_T\right]. \tag{A.7}$$

By differentiation with respect to $(1/T)$, we obtain

$$R\partial\ln Q_{den} / \partial(1/T) = R\partial\ln K_0 / \partial(1/T) - \xi_w R\partial\ln\left[(\mathrm{W}_{III})_T\right] / \partial(1/T). \tag{A.8}$$

[6] For a definition of activity and thermal equivalent dilution see Ref. [4], Appendix B.

By applying the van't Hoff Eq. (1) to Eq. (A.8), the denaturation enthalpy ΔH_{den} is obtained as

$$\Delta H_{den} = \Delta H_0 + \xi_w R\partial \ln\left[(W_{III})_T\right] / \partial(1/T). \quad (A.9)$$

The last term of this equation can be rearranged as derivative with respect to ln$T$

$$+ \xi_w R\partial \ln\left[(W_{III})_T\right] / \partial(1/T) = -\xi_w RT\partial \ln\left[(W_{III})_T\right] / \partial(\ln T) \quad (A.10)$$

and then by recalling the principle of thermal equivalent dilution (*TED*) [4]

$$-\xi_w R\partial \ln\left[(W_{III})_T\right] / \partial(\ln T) = \xi_w C_{p,w} \quad (A.11)$$

where $C_{p,w}$ is the isobaric heat capacity of water, we obtain

$$\Delta H_{den} = \Delta H_0 + \Delta C_p T = \Delta H_0 + \xi_w T C_{p,w}. \quad (A.12)$$

This means that if we plot the denaturation enthalpy against T, we should obtain a straight line with slope $\Delta C_p = \xi_w C_{p,w}$.

The passage from lnQ_{den} via Eq. (A.8) to ΔC_p of Eq. (A.12) takes place through a double derivation. In fact, the first derivative of Eq. (1) (van't Hoff equation) can be rearranged as

$$\begin{aligned} -\partial(R\ln Q_{den}) / \partial(1/T) &= -\partial(-\Delta G_{den}/T) / \partial(1/T) \\ &= -\partial(\Delta G_{den}) / (\partial \ln T) = \Delta H_{den} \end{aligned} \quad (A.13)$$

then the second derivative can be calculated as

$$\partial(\Delta H_{den}) / \partial T = -\partial^2(\Delta G_{den}) / (\partial \ln T \partial T) = \Delta C_p. \quad (A.14)$$

At the same time, however, we can calculate the entropy change ΔS_{den} as the first derivative of $-\Delta G_{den}$ as

$$\partial(-\Delta G_{den}) / \partial T = \Delta S_{den} \quad (A.15)$$

and then by recalling $dS = C_p d\ln T$, the second derivative can be calculated as

$$\partial(\Delta S_{den}) / \partial \ln T) = -\partial^2(\Delta G_{den}) / (\partial T \partial \ln T) = \Delta C_p. \quad (A.16)$$

The equality of Eq. (A.14) and Eq. (A.16) means that if we plot ΔS_{app} against ln$T$ we should obtain the same slope ΔC_p as from the function $\Delta H_{app} = f(T)$ and, therefore, we should obtain the same value of ξ_w, as already obtained in the solubilisation of inert gases($\xi_w > 0$) or in micelle formation ($\xi_w < 0$).

Appendix B. Denaturation free energy and pH

We have tried to look deeper into the problem of the determination of free energy at different pH levels and different temperatures. The equilibrium constants calculated from the actual values of free energy ΔG_{den} reported by Lumry et al. [12] are not exactly equilibrium constants, rather they are concentration quotients that are related to the equilibrium constants, with properties similar to those of the equilibrium constants. In fact, we can assume that the denaturation process is ruled by an equilibrium between denatured protein, native protein and proton. If we indicate by $[D_w]$ the concentration of the hydrated denatured protein, by $[NH_x]$ the concentration of the protonated native protein, and by $[H^+]$ the concentration of proton, the equilibrium can be written

$$D_w + xH^+ = NH_x \quad (B.1)$$

with equilibrium constant

$$K_{den} = [D_w] \times [NH_x]^{-1} \times \left[H^+\right]^x \quad (B.2)$$

which includes the constant K_{hydr} of Eq. (A.4). By considering that the protein concentration is [P] and that $[NH_x]/[P] = \alpha$ and $[D_w]/[P] = (1-\alpha)$ this expression can be rewritten as

$$K_{den} = ((1-a)/a)\left[H^+\right]^x \quad (B.3)$$

and by introducing the denaturation quotient (Fig. B.1)

$$Q_{den} = (1-a)/a \quad (B.4)$$

and rearranging, we obtain

$$\left[H^+\right]^{-x} K_{den} = Q_{den} \quad (B.5)$$

where Q_{den} is the quotient determined by Lumry [13] as free energy $\Delta G_{den} = -2.302\ RT\ \log Q_{den}$. The values of free energy reported at different temperatures for each value of pH are those around $Q_{den} = 1$.

The Eq. (B.5) shows how the ratio Q_{den} has important properties in common with the dissociation constant K_{den}. By taking the logarithm (we use the decimal logarithm in order to be on the same scale as pH) we obtain

$$\log\left[H^+\right]^{-x} + \log K'_{den} = \log Q_{den} \quad (B.6)$$

where K' is a conditional dissociation constant, holding at pH = 2.

We can show that the derivatives of both members of Eq. (B.6) with respect to temperature and pH are the same, namely

$$\partial\left(\log\left[H^+\right]^{-x}\right) / \partial \mathrm{pH} = \partial \log Q_{den} / \partial \mathrm{pH} \quad (B.7)$$

and (van't Hoff)

$$\partial \log K'_{den} / \partial(1/T) = \partial \log Q_{den} / \partial(1/T). \quad (B.8)$$

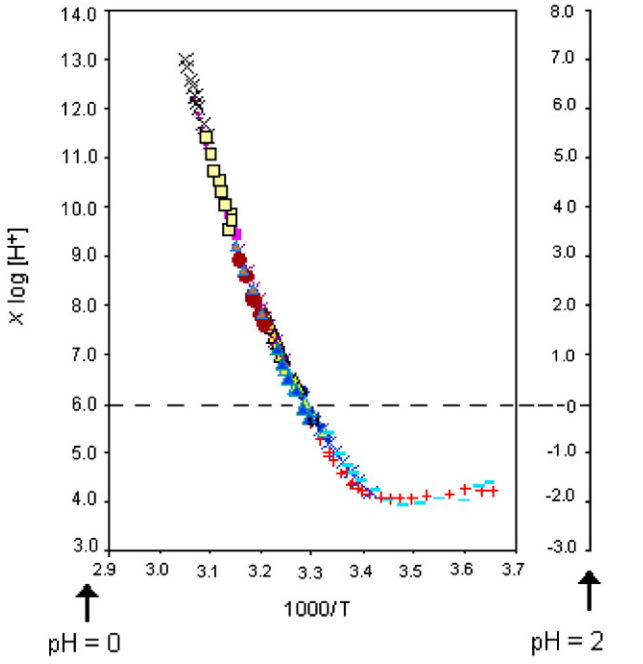

Fig. B.3. The cumulative curve obtained by displacement of each branch to pH = 0. At the right hand, the scale for displacenent to pH = 2: the curve is partially in the negative field of log Q_{den}.

Table B.1
Relationships between $\Delta(\log[H^+]^x)$ and $\Delta(pH)$ $<x> = 3.04 \pm 0.08$.

Compound	Equation		x
DMSCGN	$y = 3.16\ \Delta pH$	$+0.02$	3
CGN	$y = 2.97\ \Delta pH$	$+0.06$	3
DPC-α-CT	$y = 2.99\ \Delta pH$	$+0.09$	3
RNase	$y = 3.03\ \Delta pH$	$+0.02$	3

This derivative has been calculated in Eq. (A.8) and Eq. (A.9). The equality of Eq. (B.8) is also valid for the integrals

$$\int_{T_1}^{T_2} \partial \log K'_{den} / \partial(1/T) \mathrm{d}(1/T) = \int_{T_1}^{T_2} \partial \log Q_{den} / \partial(1/T) \mathrm{d}(1/T). \quad (B.9)$$

What means that the trend of the curve representative of $\log K_{den}$ as the function of $(1/T)$ is the same as that of $\log Q_{den} = f(1/T)$, i.e. it is a curve with a minimum.

By choosing a pH such that

$$\log\left[H^+\right]^{-x} + \log K'_{den} = 0 \quad (B.10)$$

we have $\log Q_{den} = 0$. Now, we can determine several values of $\log Q_{den}$, for example at pH = 2 (Fig. 5), around the origin O_1, by changing the temperature. We thus obtain the branch $br_{1(pH=2)}$ of the curve $\log Q_{den} = f(1/T)$. If we change pH again, we introduce a change $\Delta(\log [H^+]^{-x})$: then we can find

$$-\Delta\left(\log\left[H^+\right]^{-x}\right) = (1/2.302) \int_{T_1}^{T_2} \partial \log K'_{den} / \partial(1/T) \mathrm{d}(1/T) \quad (B.11)$$

a new value of $\log K'_{den}$ satisfying the condition of Eq. (**B.10**), if we change the temperature in such a way that $\log K_{den}$ changes by an amount exactly opposite to the variation of $\Delta(\log[H^+]^{-x})$ with pH. We now determine some values of $\log Q_{den}$ around the new origin O_2 (i.e. around $\log Q_{den} = 0$) by changing the temperature around $1/T_2$ of O_2. We thus construct the new branch $br_{2(pH=2.15)}$ around the middle point O_2 (at $\log Q_{den} = 0$) analogous to $br_{1(pH=2)}$. The trend of $br_{2(pH=2.15)}$, however, is different from the trend of $br_{1(pH=2)}$, because it is equal to that of $\log K_{den}$ (and then of $\log Q_{den}$) in a different range of higher temperatures. If we know in some way or can determine the amount of the change $\Delta(\log[H^+]^{-x})$, we can displace upward the origin of $br_{2(pH=2.15)}$ and all of its experimental points, parallel to the ordinate axis, by an amount equal to $-\Delta(\log[H^+]^{-x})$. This parallel displacement can be found graphically in such a way to insert $br_{2(pH=2.15)}$ just in continuity or in partial overlapping with the previous $br_{1(pH=2)}$. By repeating this procedure at other values of pH, we can construct the whole curve for a large interval of temperatures. Obviously, the displacement of $br_{-1(pH=1.6)}$ is downward. A schematic diagram showing the decomposition/composition procedure of the denaturation curve is shown in Fig. B.2. The cumulative function with all the curves displaced to pH = 2 is reported in Fig. B.3. If the cumulative curve is further displaced to pH = 0 the whole curve fall in the range of positive log K, thus indicating the reaction has been brought to the range where denaturation is thermodynamically favoured.

If we plot the values graphically determined of $-\Delta(\log[H^+]^{-x})$ versus $\Delta(pH)$, i.e. the variation with respect to pH = 2, we obtain the equations reported in Table B.1. From the slope of these equations, we calculate the power x, that is related to the number of protonated sites on the protein. This power results to be $<x> = 3.04 \pm 0.08$ and hence the integer 3 for every compound examined. The higher the hydrogen ion concentration added is $(\Delta(pH) < 0)$, the larger the displacement upward applied to the equilibrium constant in the diagram is. That means that the association between denatured protein and proton is increased by the addition of hydrogen ions. Alternatively to the graphical method, we can calculate mathematically the displacements of the branches, according to the following procedure. Calculate the interpolation polynomial of $br_{1(pH=2)}$ thus obtaining the function F_1 with origin O_1 and the interpolation polynomial of $br_{2(pH=2.15)}$, thus obtaining the function F_2 with origin O_2. Calculate the abscissa $1/T_1$ of O_1 and calculate the value of F_1 at this temperature T_1. This value of the function F_1 corresponds to the increment to assign to each experimental point of $br_{2(pH=2.15)}$ to bring them on the same curve of $br_{1(pH=2)}$. We compose a new cumulative branch $br_{1,2(2+2.15)}$ interpolated by a new function $F_{(1,2)}$ with origin at O_1. Then we pass to $br_{3(pH=2.4)}$ and calculate the interpolation polynomial F_3 with origin at O_3. We calculate the abscissa $1/T_3$ of O_3 and then calculate the value of the function $F_{(1,2)}$ at this point. This value is the displacement applied to all the experimental points of $br_{3(pH=2.4)}$ in order to bring them on the same curve of $br_{1,2(2+2.15)}$. We compose a new cumulative $br_{1,2,3(2+2.15+2.4)}$ for which we can calculate the interpolation function $F_{(1,2,3)}$ with the old origin O_1. We continue these steps till the last branch is included in the total set. Obviously, the displacement of $br_{-1(pH=1.6)}$ with origin at O_{-1} is negative.

References

[1] E. Fisicaro, C. Compari, A. Braibanti, Entropy/enthalpy compensation: hydrophobic effect, micelles and protein complexes, Phys. Chem. Chem. Phys. 6 (2004) 4156–4166.
[2] E. Fisicaro, C. Compari, E. Duce, A. Braibanti, Entropy changes in aqueous solutions of non-polar substances, J. Solution Chem. 37 (2008) 487–501.
[3] E. Fisicaro, C. Compari, E. Duce, M. Biemmi, M. Peroni, A. Braibanti, Thermodynamics of micelle formation in water, hydrophobic processes and surfactant self-assemblies, Phys. Chem. Chem. Phys. 10 (2008) 3903–3914.
[4] E. Fisicaro, C. Compari, A. Braibanti, Hydrophobic hydration processes. General thermodynamic model by thermal equivalent dilution determinations, Biophys. Chem. 151 (3) (2010) 119–138.
[5] J. Konicek, I. Wadso, Thermochemical properties of some carboxylic acids, amines, and N-substituted amides in aqueous solution, Acta Chem. Scand. 25 (1971) 1541–1951.
[6] H. Frank, F. Franks, Structural approach to the solvent power of water for hydrocarbons; urea as a structure breaker, J. Chem. Phys. 48 (1968) 4746–4757.
[7] S. Cabani, G. Conti, A. Martinelli, E. Matteoli, Thermodynamic properties of organic compounds in aqueous solutions. Apparent molal heat capacities of amines and ethers, J. Chem. Soc. Faraday Trans. 1 F 61 (1973) 2112–2123.
[8] E.R. Guinto, E. Di Cera, Large heat capacity change in a protein-monovalent cation interaction, Biochemistry 35 (1996) 8800–8804.
[9] R. Lumry, Uses of enthalpy–entropy compensation in protein research, Biophys. Chem. 105 (2003) 545–557.
[10] T.H. Benzinger, Thermodynamics, chemical reactions, and molecular biology, Nature 229 (1971) 100–102.
[11] D.J. Winzor, C.M. Jackson, Interpretation of the temperature dependence of equilibrium and rate constants, J. Mol. Recognit. 19 (2006) 389–407.
[12] D.F. Shiao, R. Lumry, J. Fahey, Chymotrypsinogen family of proteins. XI. Heat capacity changes accompanying reversible thermal unfolding of proteins, J. Am. Chem. Soc. 93 (1971) 2024–2035.
[13] R. Lumry, in: A. Braibanti (Ed.), Bioenergetics and thermodynamics: model systems, Interpretation of Calorimetric Data from Cooperative Systems Reidel, Dordrecht, 1980, p. 405.
[14] A. Braibanti, E. Fisicaro, C. Compari, Thermal equivalent dilution, J. Phys. Chem. B 102 (1998) 8537–8539.
[15] W. Pfeil, P.L. Privalov, Thermodynamic investigations of proteins. I. Standard functions for proteins with lysozyme as an example, Biophys. Chem. 4 (1976) 23–32.
[16] P.L. Privalov, Thermodynamic investigations of biological macromolecules, Pure Appl. Chem. 47 (1976) 293–304.
[17] J.M. Sturtevant, Biochemical applications of differential scanning calorimetry, Annu. Rev. Phys. Chem. 38 (1987) 463–468.
[18] P.L. Privalov, S.J. Gill, Stability of protein structure and hydrophobic interaction, Adv. Protein Chem. 39 (1988) 191–234.
[19] P.L. Privalov, Thermodynamic problems of protein structure, Annu. Rev. Biophys. Biophys. Chem. 18 (1989) 47–69.
[20] A. Braibanti, E. Fisicaro, Molecular thermodynamics of the denaturation of lysozyme, Thermochim. Acta 241 (1994) 131–156.
[21] S.N. Timasheff, T. Arakawa, H. Inoue, K. Gekko, M.J. Gorbunoff, J.C. Lee, G.C. Na, E.P. Pittz, V. Prakash, The role of solvation in protein stabilization and unfolding, in: F. Franks (Ed.), Biophysics of Water, J. Wiley, Chichester, 1982, p. 48.
[22] J.C. Lee, S.N. Timasheff, Partial specific volumes and interactions with solvent components of proteins in guanidine hydrochloride, Biochemistry 13 (1974) 257–265.
[23] S.N. Timasheff, Water as ligand: preferential binding and exclusion of denaturants in protein unfolding, Biochenistry 31 (1992) 9857–9864.
[24] D. Poland, Protein denaturant binding polynomials, J. Protein Chem. 21 (2002) 479–487.
[25] J.A. Schellman, Fifty years of solvent denaturation, Biophys. Chem. 96 (2002) 91–101.

[26] S. Lapaje, C. Tanford, Proteins as random coils. IV. Osmotic pressures, second virial coefficients, and unperturbed dimensions in 6 M guanidine hydrochloride, J. Am. Chem. Soc. 89 (1967) 5030–5033.
[27] Y. Qu, C.L. Bolen, D.W. Bolen, Osmolyte-driven contraction of a random coil protein, Proc. Natl. Acad. Sci. U. S. A. 95 (1998) 9268–9273.
[28] I. Baskanov, D.W. Bolen, Forcing thermodynamically unfolded proteins to fold, J. Biol. Chem. 273 (1998) 4831–4834.
[29] K. Anand, D. Pal, R. Hilgenfeld, An overview on 2-methyl-2,4-pentanediol in crystallization and in crystals of biological macromolecules, Acta Crystallogr. D58 (2002) 1722–1728.
[30] E.A. Galinski, M. Stein, B. Amendt, M. Kinder, The kosmotropic (structure-forming) effect of compensatory solutes, Comp. Biochem. Physiol. A Physiol. 117 (1997) 357–365.
[31] R. Koynova, J. Brankov, B. Tenchov, Modulation of lipid phase behaviour by kosmotropic and chaotropic solutes, Eur. Biophys. J. 25 (1997) 261–274.
[32] D.B. Wetlaufer, S.K. Malok, L. Stoller, R.L. Coffin, Nonpolar group participation in the denaturation of proteins by urea and guanidinium salts. Model compound studies, J. Am. Chem. Soc. 86 (1964) 508–514.
[33] D.T. Haynie, Biological Thermodynamics, Cambridge Univ Press, Cambridge, 2001, p.169.
[34] N. Pace, C. Tanford, Thermodynamics of the unfolding of beta-lactoglobulin A in aqueous urea solutions between 5 and 55 degrees, Biochemisry 7 (1968) 198–208.
[35] F. Vanzi, B. Madan, K. Sharp, Effect of the protein denaturants urea and guanidinium on water structure: a structural and thermodynamic study, J. Am. Chem. Soc. 120 (1998) 10748–10753.
[36] K.A. Sharp, B. Madam, Hydrophobic effect, water structure, and heat capacity changes, J. Phys. Chem. 101 (1997) 4343–4348.
[37] B. Widom, P. Bhimalapuram, K. Koga, The hydrophobic effect, Phys. Chem. Chem. Phys. 5 (2003) 3085–3093.
[38] P.J. Rossky, Protein denaturation by urea: slash and bond, Proc. Natl. Acad. Sci. U. S. A. PNAS 105 (2008) 16825–16826.
[39] D. Chandler, Insight review: interfaces and the diving force of hydrophobic assembly, Nature 437 (2005) 640–647.
[40] S. Rajamani, T.M. Truskett, S. Garde, Hydrophobic hydration from small to large length scales: understanding and manipulating the crossover, PNAS 102 (2005) 9475–9480.
[41] K. Lum, D. Chandler, J.D. Weeks, Hydrophobicity at small and large length scales, J. Phys. Chem. B 103 (1999) 4570–4577.
[42] V.V. Yaminsky, E.A. Vogler, Hydrophobic hydration, Curr. Opin. Colloid Interface Sci. 6 (2001) 342–349.
[43] H.S. Frank, M.W. Evans, Free volume and entropy in condensed systems. III, Entropy in binary liquid mixtures; partial molal entropy in dilute solutions; structure and thermodynamics in aqueous electrolytes, vol. 13, 1945, pp. 507–532.
[44] G. Nemethy, H.A. Scheraga, Structure of water and hydrophobic bonding in proteins. I. A model for the thermodynamic prperies of liquid water, J. Chem. Phys. 36 (1962) 3382–3400.
[45] G. Graziano, A van der Waals approach to the entropy convergence phenomenon, Phys. Chem. Chem. Phys. 6 (2004) 406–441.
[46] Y.-D. Linney, R. Edelman, I. Kusner, R. Kisillak, S. Srebic, Water structure effect of sugar stereochemistry and its impact on protein thermal stability, Frontiers in Water Biophysics, May 23–26 2010, Trieste.

Glossary

Class A: Processes with transformation $\mathbf{A}(-\xi_w W_I \rightarrow \xi_w W_{II} + \xi_w W_{III} + \text{cavity})$
Class B: Processes with transformation $\mathbf{B}(-\xi_w W_{III} - \xi_w W_{II} \rightarrow \xi_w W_I - \text{cavity})$
W_I: water cluster $(W_5)_I$,
W_{II}: water cluster $(W_4)_{II}$
W_{III}: free water molecule
$\pm\Delta W_I$: water W_I changing to form or reduce cavity
$+\xi_w$: number of water molecules W_{III} expelled from cavity
$-\xi_w$: number of water molecules W_{III} restructured to reduce cavity
TED: thermal equivalent dilution (Ergodic Hypothesis)
FCB: Fisicaro, Compari, Braibanti
ΔH_{app}: apparent enthalpy (experimental enthalpy in a general hydrophobic process)
ΔH_{den}: denaturation enthalpy ($\equiv\Delta H_{app}$)
$\Delta H_{(0)}$: ΔH_{den} extrapolated to $T=0$
ΔH_{mot}: motive component of enthalpy ($\equiv \Delta H_{(0)}$)
ΔH_{den}: $\Delta H_{mot} + \Delta H_{therm}$
ΔH_{therm}: thermal component of enthalpy ($= +\Delta C_p\, T$ in Class A)
ΔH_{mot}: $\Delta H_0^{(\xi_w=0)} + \Delta H_{for}$
$\Delta H_0^{(\xi_w=0)}$: ΔH_{mot} extrapolated to $\xi_w = 0$ (no cavity, $\Delta H_{for} = 0$)
$\Delta H_{for}<0$: $\xi_w \cdot \Delta h_{for}$ enthalpy change for cavity formation
Δh_{for}: $-22.5\ \text{kJ}\cdot\text{mol}^{-1}\cdot\xi_w^{-1}$, unitary enthalpy change for cavity formation
$\Delta H_{red}>0$: $\xi_w \cdot \Delta h_{red}$ enthalpy change for cavity reduction
Δh_{red}: $+22.5\ \text{kJ}\cdot\text{mol}^{-1}\cdot\xi_w^{-1}$, unitary enthalpy change for cavity reduction
ΔS_{app}: apparent entropy (experimental entropy in a general hydrophobic process)
ΔS_{den}: denaturation entropy ($\equiv\Delta S_{app}$)
$\Delta S_{(0)}$: ΔS_{den} extrapolated to $\ln T = 0$
ΔS_{mot}: motive component of entropy ($\equiv \Delta S_{(0)}$)
ΔS_{den}: $\Delta S_{therm} + \Delta S_{mot}$
ΔS_{therm}: thermal component of entropy ($= +\Delta C_p \ln T$ in Class A)
ΔS_{mot}: $\Delta S_0^{(\xi_w=0)} + \Delta S_{for}$
$\Delta S_0^{(\xi_w=0)}$: ΔS_{mot} extrapolated to $\xi_w = 0$ (no cavity, $\Delta S_{for} = 0$)
$\Delta S_{for}<0$: $\xi_w \cdot \Delta s_{for}$, entropy change for cavity formation
Δs_{for}: $-445 \pm \Delta\ \text{J}\cdot\text{K}^{-1}\cdot\text{mol}^{-1}\cdot\xi_w^{-1}$, unitary entropy change for cavity formation
$\Delta S_{red}>0$: $\xi_w \cdot \Delta s_{red}$, entropy change for cavity reduction
Δs_{red}: $+432 \pm \Delta\ \text{J}\cdot\text{K}^{-1}\cdot\text{mol}^{-1}\cdot\xi_w^{-1}$, unitary entropy change for cavity reduction
ΔC_p: $+\xi_w C_{p,w}$, slope of the plot $\Delta H_{den} = f(T)$, (Class A, $\Delta C_p > 0$)
ΔC_p: $+\xi_w C_{p,w}$, slope of the plot $\Delta S_{den} = f(\ln T)$ (Class A, $\Delta C_p > 0$)
ΔC_p: $-\xi_w C_{p,w}$ (Class B, $\Delta C_p < 0$)
$C_{p,w}$: $75.36\ \text{J}\cdot\text{K}^{-1}\text{mol}^{-1}$, isobaric heat capacity of liquid water
ΔG_{mot}: motive free energy ($\Delta G_{mot} = \Delta H_{mot} - T\Delta S_{mot}$)
ΔG_{fold}: folding free energy ($\equiv\Delta G_{mot}$)
ΔG_{den}: denaturation free energy($\equiv\Delta G_{mot}$)
$\Delta G_{den}{}^{\circ}$: denaturation free energy at $c = 0$ denaturant
ΔG_{unfold}: unfolding free energy ($\equiv\Delta G_{mot}$)
ΔG_{therm}: thermal free energy $= 0$ ($\Delta H_{therm} = T\Delta S_{therm}$)
K_{den}: denaturation equilibrium constant
CGN: chymotrypsinogen A
DMSCGN: dimethionine sulfoxide derivative of chymotrypsinogen A
DPC-α-CT: diphenyl-carbamyl-α-chymotrypsin
RNase: ribonuclease
MPD: 2-methyl-2,4-pentanediol
TMAO: trimethylamine-N-oxide
$\xi_w(H)$: ξ_w calculated from the enthalpy plot
$\xi_w(S)$: ξ_w calculated from the entropy plot
K_{for}: equilibrium constant for cavity formation
K_{prot}: equilibrium constant for protonation
K_{den}: denaturation constant $= K_{for} \cdot K_{prot}$
HEW: hen egg-white lysozyme
IC: isothermal calorimetry
DSC: differential scanning calorimetry
RNM: random network model
θ_h: hydrogen bond angle
T_{den}: denaturation temperature
$dV_{for}>0$: change in volume in cavity formation
GuHCl: guanidinium hydrochloride
$<\Delta h_{for}>_A$: $-22.2 \pm 0.7\ \text{kJ}\cdot\text{mol}^{-1}\cdot\xi_w^{-1}$, mean value in Class A
$<\Delta s_{for}>_A$: $-445 \pm \Delta\ \text{J}\ \text{K}^{-1}\cdot\text{mol}^{-1}\cdot\xi_w^{-1}$ mean value in Class A,
$<\Delta h_{red}>_B$: $+23.7 \pm 0.6\ \text{kJ}\cdot\text{mol}^{-1}\cdot\xi_w^{-1}$, mean value in Class B
$<\Delta s_{red}>_B$: $+432 \pm \Delta\text{J}\ \text{K}^{-1}\cdot\text{mol}^{-1}\cdot\xi_w^{-1}$ mean value in Class B
Q_{conf}: conformational transition N → D
Q_{den}: denaturation quotient = [D]/[N]
$-\xi_w\, RT\, \partial ln[(W_{III})_T]/\partial(lnT)$: change of activity of W_{III} by temperature